Thesis for the degree
of Candidatus Scientiarum
Anja Michaelsen

Interactions between HMHEC and mono- and bisquaternary ammonium bromide surfactants in aqueous solutions.

DEPARTMENT OF CHEMISTRY
FACULTY OF MATHEMATICS
AND NATURAL SCIENCES
UNIVERSITY OF OSLO 3/2003

1 ABSTRACT

Two bis (quaternary ammonium bromide) surfactants, hexanediyl-1,6-bis(dimethyldodecylammonium bromide) (12-6-12) and dimethylparaphenyl-α,ω-bis(dimethyldodecylammonium bromide) (12-φ-12), were synthesised and their degree of solubility in water and melting point were compared. Hydrophobically modified HEC was synthesised from HEC and bromo tetradecane in an homogeneous reaction. The degree of hydrophobically modification of the synthesised HMHEC 2 was compared with a commercially HMHEC by capillary viscosimetry measurements.

The interactions in aqueous solutions of hydrophobically modified HEC (HMHEC) with the dimeric surfactant hexanediyl-1,6 bis (dimethyldodecyl ammonium bromide) (12-6-12, fig 1c)) and the single chained analogue dodecyltrimethylammonium bromide (DoTAB), were investigated by shear viscosimetry and capillary viscosimetry. From the measurements in capillary viscosimetry, intrinsic viscosity [η] and Huggins constant k_H were estimated and plotted against concentration of surfactant. The measurements were performed on solution in the dilute regime of HMHEC, where the polymer exist as individual, or partially overlapping coils, due to interassociation between the hydrophobes on HMHEC. [η] showed a strong decrease and k_H showed a strong increase below CMC and the opposite behaviour above CMC as a function of surfactant concentration. Both systems of HMHEC with surfactant revealed phase-separation in a region around CMC, due to very strong intermolecular interactions. High values of k_H revealed strong interactions in both systems of HMHEC with DoTAB and 12-6-12. The highest values and a more co-operative pattern of [η] and k_H in surfactant concentration were found in the HMHEC/12-6-12 system.

The measurements in rheology on semidilute aqueous solutions of HMHEC with surfactant showed shear thinning behaviour for both DoTAB and 12-6-12. The value of zero-shear viscosity η_0 at maximum, occurring around CMC for both HMHEC/12-6-12 and HMHEC/DoTAB, was the highest for HMHEC/DoTAB. The shear thinning started at the highest shear rate for the HMHEC/12-6-12 system.

2 INTRODUCTION

Hydrophobically modified hydroxyethylcellulose, HMHEC, is a graft-modified polymer, where the hydrophobic groups (alkylchains) are grafted onto the HEC backbone as side groups. HMHEC has an amphiphilic character, and is composed of hydrophobic groups and a more polar polymer backbone. The latter make HMHEC a water-soluble polymer (wsp), which self-associates in water through interactions between the hydrophobic groups in nodular domains[1].

HMHEC are used in many areas, such as rheology modifier in latex paints, thickener in shampoo, as stabiliser in emulsion polymerisation of vinyl and allylic monomer, as emulsifier in cosmetic lotions due to its ability to reduce interfacial tensions, and as thickener in enhanced oil recovery [2].
Above a critical polymer concentration c* (overlap concentration, 3.4.2.), wsp form an associated network in water. Hydrophobically modified (hm) polymers associate through the hydrophobic groups in micelle-like aggregates which form junction zones in the physical network.. These associations lead to a marked increase in the solution viscosity[2]. Below c*,

the association of hm-polymer occur intramolecularly within the polymer coils. Hydrophobic groups on the same polymer chain tend to cluster, to disrupt the water structure as less as possible[2]. Intermolecular association can occur at elevated polymer concentrations below c* through association between hydrophobic groups on different polymer molecules to form aggregates. The size of the polymer coils can be described by intrinsic viscosity [η], which is a specific volume of the individual polymer molecules (3.4.2.)[3].

Addition of ionic surfactant to aqueous solutions of hm-polymers yields a modulation of the viscosity and the thermodynamics of the solution due to association between surfactant and polymer. The surfactant adds to the hydrophobic domains on the polymer and form mixed micelles with the hydrophobic groups on the polymer when the concentration is above c*. The formation of mixed micelles is thermodynamic preferable, by a lowering in the free energy of the hydrophobic junctions by less water contact[4]. The concentration that marks the onset of association between polymer and surfactant in water, CAC (critical aggregation concentration)[5] is low in the case of hm-polymer with ionic surfactant[1].

Several results[3,6,7,8,9] reports on modulation of viscoelastic properties as viscosity on addition of ionic surfactant to aqueous solutions of hydrophobically modified polymer. Nilsson et al. performed capillary viscosimetric measurements on dilute solutions of hydrophobically modified EHEC, HMEHEC, with added SDS[3]. They found that the viscosity decreased at low SDS concentration to a minimum, and thereafter increased in increasing SDS concentration. The decrease in viscosity is explained in two ways. In the dilute solutions of HMEHEC, the viscosity describes the size of the polymer coils in solutions, and addition of ionic surfactant lead to an increase in intramolecular interactions and thereby to a decrease in viscosity and coil size. Eventually, there exist aggregates of HMEHEC and SDS at low SDS concentrations, which disintegrate at higher SDS-levels, giving a decrease in viscosity. The minimum in viscosity is related to the critical aggregation concentration CAC, and the following increase in viscosity is due to a progressive binding of SDS to HMEHEC, which make the polymer swell and make it more extended.

Panmai et al.[7] performed steady-shear viscosity measurements on semidilute aqueous solutions of HMHEC modified with C_{16} alkyl chains with the cationic surfactants CTAB and TTAB. They found that the viscosity increased to a maximum and then decreased in increasing the surfactant concentration in the HMHEC solutions. The maximum appeared somewhat above cmc of both CTAB and TTAB. Also steady-state fluorescence-experiments were carried out to estimate the aggregation number and composition of the mixed micelles with increasing surfactant concentration. The results show a decrease in the number of hydrophobes per mixed micelle from $N_H \approx 3$ at no added surfactant to $N_H \approx 2$ at the viscosity maximum. This is explained by a transition at $N_H = 2$ from bridging ($N_H > 2$) to masking ($N_H < 2$) of the hydrophobe clusters by surfactant.

Gemini (dimeric) surfactants are composed of two amphiphilic parts, connected by a spacer group at the level of the end groups[10] (fig. 1b)). Dimeric surfactants with a hydrophobic spacer chain are more hydrophobic than monomeric surfactants with the same length of the alkyl chains[11], which can induce stronger interactions between dimeric surfactant with hm polymer. The polymer-surfactant-interactions are revealed to be stronger for the case of dimeric surfactant than with monomeric surfactant[10,12,13].

Bai et al.[13] performed isothermal microcalorimetric measurements on aqueous solutions of copolymers and terpolymers of acrylamide, N,n-alylacrylamide and acrylic acide with 12-3-

Figure 1: Dash formulas for a) Dodecyltrimethylammonium bromide, b)12-6-12, c)12-φ-12, d) m-s-m (general formula)

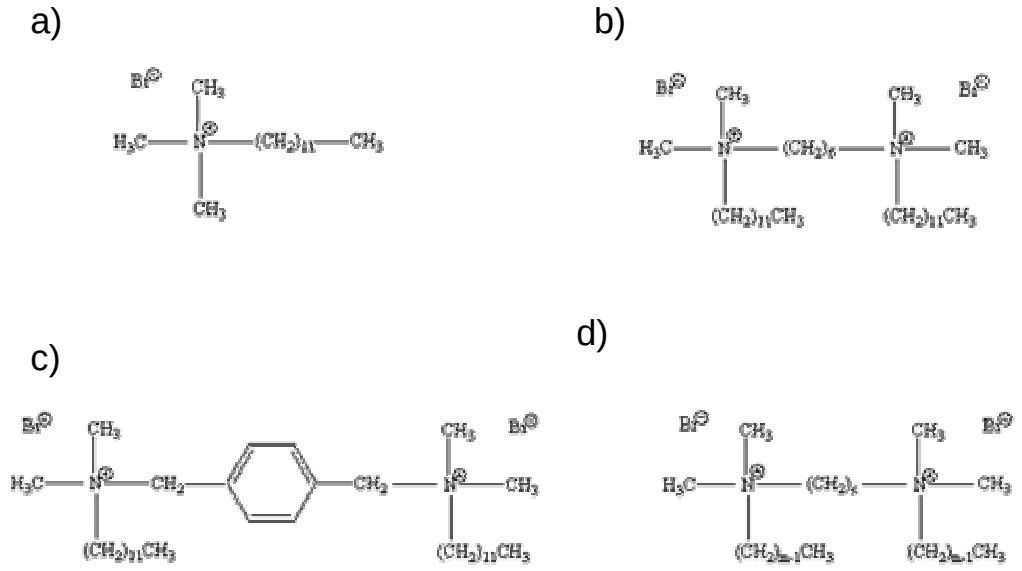

12, 12-6-12 and DoTAB. They measured the enthalpy difference of adding surfactant to polymer solution. By subtracting ΔH for addition of surfactant to pure water, they found $\Delta H = \Delta H_{ps}$ of the process polymer + free surfactant micelle $\rightarrow$ polymer-bound micelle. The value of ΔH_{ps} was positive, and much larger for 12-6-12 than for DoTAB, indicating stronger interactions for 12-6-12 with polymer. ΔH_{ps} was endothermic for all samples of polyacrylamide with hydrophobic substitution and surfactant. Values of $T \cdot \Delta S$ was calculated through expressions for ΔG and the measured ΔH. The entropy of interaction ΔS_{ps} of polymer and surfactant was found to be positive, and hence the aggregation of surfactant on polymer was entropy-driven. ΔS_{ps} of 12-6-12 with polymer was higher than for DoTAB with polymer, and hence the interaction between polymer and surfactant was most entropically favourable in the case of 12-6-12. Isothermal calorimetrical studies of interactions between hydrophobically modified HASE-polymers with SDS showed that the polymer-surfactant-interaction was entropy-driven, and that ΔS increased with increasing hydrophobicity of the HASE-polymer[14]. Pisarcik et al. reports on interactions between hyaluronate-NaCl and both DoTAB and 12-s-12 surfactants. The structure of the backbone of hyaluronic acid is similar to that of HMHEC. They found that the interactions between the polymer hyaluronate and 12-s-12 occurred for lower surfactant concentrations than with hyaluronate and DoTAB. They also found that NaCl screened the interactions in the system with DoTAB, but not in the system of hyaluronate and 12-s-12, indicating stronger associations between 12-s-12 and hyaluronate than between DoTAB with hyaluronate[15].

In this work, hydrophobic association in aqueous solution was compared for HMHEC with DoTAB and hexanediyl-1,6-bis(dimethyldodecylammonium bromide) (12-6-12). The interactions were studied by measurements in capillary viscosimetry and shear viscosimetry. 12-6-12 is a bis (quaternary ammonium bromide) surfactant (fig. 1b), a group of surfactant that has gained certain interest in recent time[10-13,16-19,24-27,30-33,35,36] due to unusual properties in aqueous solution.

3 THEORY

3.1 Gemini surfactants

3.1.1 alkanediyl-α,ω-bis(dimethyldodecylammonium bromide) (m-s-m) surfactants and dodecyltrimethylammonium bromide (DoTAB)

The critical aggregation concentration CMC is defined as the concentration of surfactant at which the surfactant monomer form aggregates (micelles) in water[23]. CMC of m-s-m surfactants are 10 to 100 times lower than cmc of the corresponding monomeric surfactant[10]. The lower CMC for m-s-m surfactants (figure 1 b)) is partly due to incorporation of a hydrophobic spacer group, which increases the overall hydrophobicity of the surfactant[11].

12-6-12 is a bis (quaternary ammonium bromide) surfactant, generally termed m-s-m, where m and s are the number of C-atoms in the alkyl chains and the spacer, respectively. DoTAB is the analogue, single chain surfactant to 12-6-12, with the same alkyl chain length as 12-6-12. The value of CMC of 12-6-12 (1,09±0,04 mmolar[15]) is not so much lower than cmc for DoTAB (16 mmolal)[24,25]. The lower CMC for 12-6-12 than for DoTAB, is related to the higher hydrophobicity of 12-6-12 due to the hydrophobic spacer group[11], which increases the overall hydrophobicity of the surfactant and thereby its ability to aggregate in water.
The value of CMC as function of s for 12-s-12 is at a maximum[10,26,27] around s =6. The increase in CMC for m-s-m with s up to s=6 is due to conformation changes for 12-s-12 induced by the spacer. It changes from trans/gauche to cis upon increasing s due to steric hindrance of the alkylchains at short spacer length. The cis conformation lead to an increased interaction between the alkyl chains, which gives a less negative ΔG of micellisation, and a higher CMC[27]. For m-s-m surfactants with s ≤5, the spacer length is shorter than the equilibrium distance between the headgroups[24], which causes repulsion between the headgroups within the molecule. The repulsion leads to a smaller headgrouparea per molecule and closer packing of the molecules in the micelles[25], and to micellar aggregates with lower curvature[24,18] than spherical.
The CMC of the geminisurfactants decrease with increasing length of the hydrocarbon chain, as for monomeric surfactants[26]. For m-s-m surfactants with s≥14, the long spacer loops and sticks between the alkylchains in the micelles to prevent water contact. As a result, the surfactant forms vesicles, aggregates of low curvature[24].

Ion pairing is observed for 12-6-12 by neutron reflectivity by Li et al. at low concentration below CMC. Ion pairing involves binding of counterions to ions in a solvent. Li et al. found that the dissociation of 12-6-12 in water decreased from 3 species at low concentration to 2 species at higher concentrations, below CMC[10]. 12-s-12 surfactants lack a lot of the properties related to dimeric surfactants. Ion pairing[10] occur for m-s-m with m around 8-10, premicellar aggregation[10] is observed for m≥16 and for s>12. Premicellar aggregation, which

can be caused by ion pairing, involves than the surfactant form aggregates of low aggregation number below CMC[12]. Ageing effects (slow kinetics of the surfactant) and self-coiling of the alkylchains occur for long alkylchains[10]. The headgroup distance in 12-6-12 is near the thermodynamic equilibrium distance 7-9 Å between headgroups in micelles of conventional single chain analogues[10]. This leads to more flexible spacer[29] and less headgroup-repulsion internal in the molecule of 12-6-12 than for shorter spacer-lengths. This make the properties of 12-6-12 nearer those of DoTAB than for shorter spacers. Both 12-6-12[10,17,19,29] and DoTAB form spherical micelles around CMC. The aggregation number of DoTAB[30,31] (N_{agg}: 61, 70±5) is a little higher than that of 12-6-12[29] (N_{agg} : 54) reported as number of dodecylchains per micelle. For both DoTAB and 12-6-12 the aggregation number is almost constant[29,30] in concentration of the surfactant. The surface area per dodecylchain at CMC for DoTAB[32] (48 $Å^2$) is near that for 12-6-12[32] (49 $Å^2$). 12-6-12 is reported to form larger micelles in water than DoTAB, which give a lower surface-charge-density to micelles of 12-6-12[15]. The aggregation number of 12-6-12 in aqueous solution of triblock copolymers of PPO and PEO showed small dependency of polymer-concentration, and were lower than in pure water[20]. The large aggregation number indicates a co-operative micellisation for both 12-6-12 and DoTAB[25].

3.1.2 hexanediyl-1,6-bis(dimethyldodecylammonium bromide) (12-6-12) and dimethylparaphenyl-α,ω-bis(dimethyldodecylammonium bromide) (12-φ-12)

Polymethylene spacers as in 12-6-12 and paraphenyl-spacers in 12-φ-12 are classified as flexible and rigid, respectively[33]. The flexibility of the spacer infects properties as CMC and solubility in water. The surface-activity of gemini surfactant, increases with increasing flexibility of the spacer, and bulky or rigid spacers create a larger surface tension[34].
More rigid spacers give higher cmc to the surfactant[25]. CMC is a little higher for 12-φ-12[32,35] (1,2 mmolal) than of 12-6-12[36] (1,09±0,04 mmolar) .The solubility of dimeric surfactants with rigid spacer is lower than for dimeres with flexible spacer[33]. The phenyl-ring in 12-φ-12 possibly reduces the solubility of the surfactant more than the hexamethylene-spacer in 12-6-12. Benzene has a low solubility in water, due to a large negative ΔS of solubilisation in accordance with high degree of ordering of water molecules around benzene[37].

The spacer is fully extended on the micellar surface[29] for m-s-m surfactants when s<6 . The spacer conformation of 12-6-12 is thereby fairly linear, so the spacer is possibly stretched out on the micellar surface for both 12-6-12 and 12-φ-12[36].
The distance between the headgroups for both 12-6-12[29] and for 12-φ-12[33] is around the thermodynamic equilibrium distance[10] 7-9 Å, evaluated for micelles of conventional monomeric quaternary ammonium surfactants. The surface area per dodecylchain at cmc of 12-6-12 and 12-φ-12 are 49 $Å^2$ (25°C, cmc) and 48 $Å^2$(40°C, cmc), respectively[32]. The headgroup-areas of 12-6-12 and 12-φ-12 are 1,51±0,08nm^2 and 1,7± 0,3 nm^2, respectively[36]. 12-6-12 is reported to form spherical micelles (see 3.1.2.), but 12-φ-12 form small aggregates of aggregation number 2 (c ≈ cmc) and 4 at (c ≈ 4·cmc) in solutions of 0,1 M NaCl. Conductivity measurements on 12-φ-12 and 12-6-12 show no premicellar aggregation or ionpairing[12].

3.2 ^{1}H-NMR

In NMR, properties of nuclei that possess a magnetic moment are studied by application of a magnetic field and study the resonant electromagnetic field.

NMR observable nuclei have I≠0 and the angular momentum of a nuclei is $hI(I+1)^{½}/2\pi$, where h is Planck's constant. In ^{1}H NMR, the signal from protons (^{1}H, I=½,) is observed

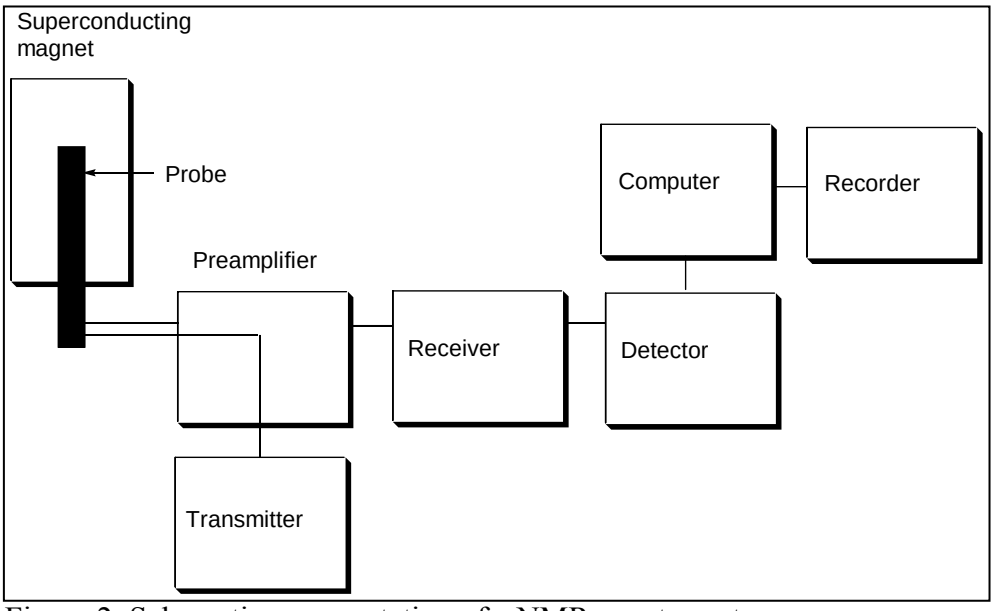

Figure 2: Schematic representation of a NMR-spectrometer.

3.2.1 The technique

In solution ^{1}H NMR, the sample is dissolved in a deuterated solvent in a glass capillary tube with outer diameter 5 mm[38]. A schematic representation of a NMR spectrometer[38] is shown in figure 2. The sample is placed in a cylindrical wound magnet and the sample is sometimes rotated to make the magnetic field more homogeneous. The magnet is a permanent magnet or a superconducting magnet (for higher magnetic fields). Superconducting magnets are cooled by He (l) and keeps a temperature of 4K. The measurement is performed at room temperature or a decided temperature[39]. A pulse of radiofrequent radiation is sent to the probe, and the weaker output signal is enhanced by a preamplifier. The signal is then sent through a transmitter to a detector, where the signal is fouriertransformed into a frequency dependent signal (FID), then converted from analog to digital, and then stored in the computer.
The signal with low intensity from the preamplifier is sent through the receiver where it is amplified, before it enters the detector[38].

3.2.2 Resonance[39]

The magnetic quantum number m_I have the values I, I-1, …, -I , and each value corresponds to a direction (2I+1 orientations) of the nuclear magnetic moment μ. The z-component of μ is proportional to the z-component of the spin angular moment in the z-direction ($m_I h/2\pi$):

1) $\mu_z = \gamma h m_I/2\pi$

γ is the magnetogyric ratio[39]. A nucleus in an external magnetic H_0 field in the z-direction have energy levels $E = -\mu_z H_0 = (\gamma h m_I/2\pi)*H_0$. Nucleus with I=1/2 are splitted (Zeeman splitting[38]) into energy levels $E = \pm½*(\gamma h/2\pi)*H_0$. The nucleus come into resonance with the external field when the energy of the electromagnetic radiation ($E=h\nu$) equals the difference in the energy levels ($\gamma h H_0/2\pi$) of the nucleus. (Bohr condition)[38], which gives

2) $\nu_L = \gamma H_0/2\pi$

Where ν_L is the Larmor frequency[39]. At resonance conditions, the nucleus adsorbs much energy due to the change in spin, which give strong coupling between the nucleus .The population of the energy levels is given by the Bolzmann distribution:

3) $N_\beta/N_\alpha = \exp(-\Delta E/k\cdot T)$

Where N_β and N_α is the population of the higher and lower energy level, respectively. The signal intensity is increased by increasing the field strength of the applied magnetic field (H_0) through an increase in the energy absorbed by the nucleus, and increasing the difference in the population of the spinstates (lowering in N_β/N_α) .

When the probe is placed in a magnetic field H_0, the nuclei experience a lower field strength H', due to shielding by the electrons around it, $H' = (1-\sigma)\, H_0$.
σ (shielding constant) depends on the spatial arrangement of the electrons around the nuclei and on the molecular environment. σ is a tensor, and the constant is the average of the principal values of the tensor. The frequency (resonance frequency) of the absorbed energy for a nucleus, ν_{sample}, is determined by the electronic environment of the nuclei. The difference between ν_{sample} and the resonance frequency of a standard, $\nu_{standard}$, gives the chemical shift (δ) of the nuclei, $\delta = 10^6\cdot(\nu_{sample}-\nu_{standard})$. In ^{1}H NMR, the NMR-spectrometer is calibrated with TMS (tetramethylsilane) as a standard[40]. The shift value (in Hz or ppm) determines the position of the intensity peak of a nucleus in the NMR spectrum. Less shielded nuclei appears to the right in the spectrum[38]. Protons bound to benzene ($\delta\approx$7-8ppm) are deshielded by the ring current which is induced when the applied magnetic field is perpendicular to the planar ring, and benzene protons are shifted to high ppm-values. Protons connected to O-atoms (f.ex. OH-groups) are deshielded ($\delta\approx$4) due to the electronwithdrawing effect of oxygen[39].

3.2.4 Spin-spin-coupling[38]

The intensity peaks in the ^{1}H NMR spectrum are also splitted due to interaction between the neighbouring nuclei through the binding electrons of the nuclei (spin-spin-coupling). Interactions between two nuclei with one, two, bonds between them is called one-bond, two-bond spin-spin-coupling, respectively, and the coupling strength decreases with the number of bonds between the interacting nuclei[38]. The intensity peak for protons bound to an atom adjacent to an atom bound to n protons, is splitted into n+1 lines. The intensity distribution of the lines for a peak is given by Pascal's triangle[39].

3.2.5 Dipolar coupling[38]

The nuclei also couple direct through space (dipolar coupling),by interactions between the local magnetic field of each nuclei. The interaction strength depends on the distance between the nuclei and the angle between the direction of H_0 and the position vector between the nuclei. Dipolar coupling leads to a broadening of the intensity peaks in the NMR spectrum, and is a tool in measuring the distances between the nuclei in a compound.

3.2.6 The ^{1}H NMR spectrum[38]

A ^{1}H NMR-spectrum show relative intensity of the signal as a function of chemical shift (δ). A peak in the spectrum corresponds to the signal from protons in the same chemical environment. The integral of a peak relative to another peak give the relative amount of protons from the chemical environments represented by each peak. Peak-integration is a tool to reveal the chemical structure of a compound. The position of a peak (shift,δ) depends on the electron environment around the proton.

The shifts of the protons also depend on the protons connected to the neighbour atom by coupling (3.2.4.). The coupling lead to peak splitting, each peak is splitted into n+1 peaks, n = the number of the protons on the neighbour atom. Peak splitting is due to splitting of the energy levels for a proton, influenced by the magnetic field from the protons on adjacent atoms. The peaks are termed: singlet (no splitting), doublet (splitting into two peaks), triplet (splitting into three peaks), multiplets (splitting into more than three peaks).

The component to be analysed by ^{1}H NMR, is dissolved in a deuterated solvent, to prevent signal from solvent-protons.

3.3 Mass Spectrometry[41,40]

MS is a sensitive method, for analysing solids and liquids. The principle is formation of ions in the gas-phase, which are accelerated in an electric field, and then separated, by difference in mass[7].

3.3.1 ESI (Electrospray Ionization)[7]

In pneumatically assisted Electrospray ionisation (figure 3) the compound is dissolved in a solvent, where it is dissociated into ions, is protonated or form a charged complex with either solvent or ionic impurities in solution (ex. NH_4^+, HCO_2^-, $CH_3CO_2^-$, Na^+, H^+). The solvent is e.g. water. The method involves very little fragmentation of the compound.

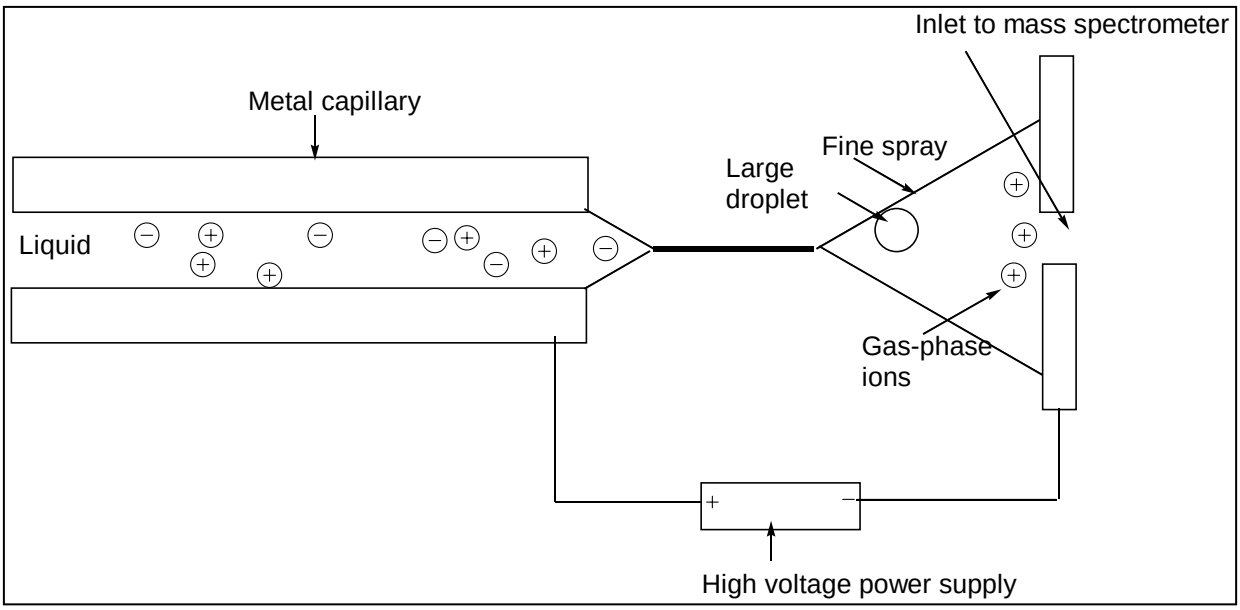

Figure 3: Schematic representation of Electrospray Ionisation.

The sample flow through a metal capillary together with a nebulizing gas (N_2). The ionic species in the solution are accelerated by an electric field potential over the capillary.
The potential over the capillary form the sample and the nebulizing gas into a aerosol of charged droplets at the end of the capillary (electrospay). The solvent evaporates, and the ionic species from the solution are in gas phase. The charge of the aerosol is positive if the voltage is positive at the outlet of the capillary. The electrospray-method does not create new ions, but transfers existing ions to gas-phase.

3.3.2 Time Of Flight mass spectrometer[7]

In a time-of flight (TOF) mass spectrometer (figure 4), a grid voltage accelerates the ions, giving the ions a constant kinetic energy. The ions enter a drift tube, where the ions are separated due to different mass, the higher mass ions have the lowest velocities.

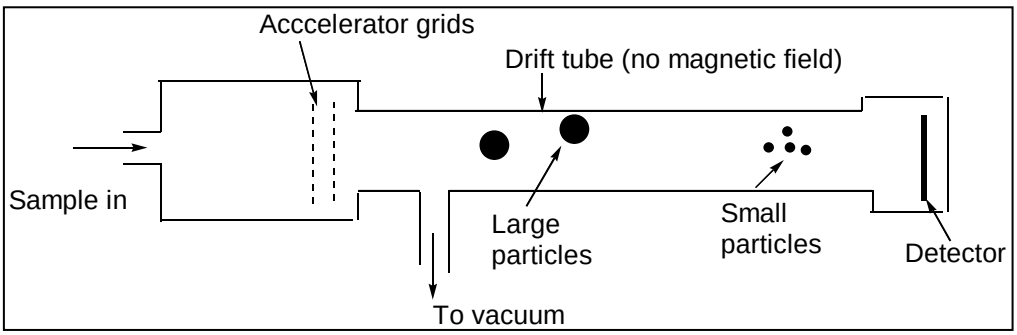

Figure 4: Schematic representation of a "Time Of Flight" (TOF) mass separator.

The energy given due to the applied electric field is

4) $E = z \cdot e \cdot V$

Where z is the valence of the ion, e is the elementary charge and V is the applied electric field. The energy is transferred to kinetic energy = $\frac{1}{2}mv^2$, where m and v are the mass and velocity of an ion, respectively. The velocity of the ion in the drift tube becomes:

5) $v = (2*z*e*V/m)^{1/2}$

The speed of the ions in the drift tube depends on m/z, with decreasing v with increasing m/z.The ions are detected as a current as a function of time by a detector in the end of the drift tube.
"Time-of-flight" give high sensitivity, high resolution and high mass-accuracy.

3.3.3 Quadruple mass spectrometer[7]

With a quadrupole mass spectrometer, gaseous ions are accelerated by an electric field, and then enter a quadrupole mass separator. The separator consists of four parallel metal rods, over the separator it is applied both a constant voltage and a oscillating voltage. The gaseous ions enter the separator and travel along the metal rods and hit an ion detector in the other end of the path. Each value of the voltage allows only ions with one m/z-value to reach the detector. The voltage over the metal rods is rapid changed in time.

3.4 Capillary viscosimetry

3.4.1 Reduced viscosity[23]

In capillary viscosimetry, viscosity is obtained by measurement of time of flow for a solution through a thin glass capillary. For a Ubbelohde viscometer (figure 5), the solution flow vertically through the capillary, only driven by the weight ρgL of the solution, where ρ is the density of the solution, g is the gravitational constant, and L is the length of the capillary.

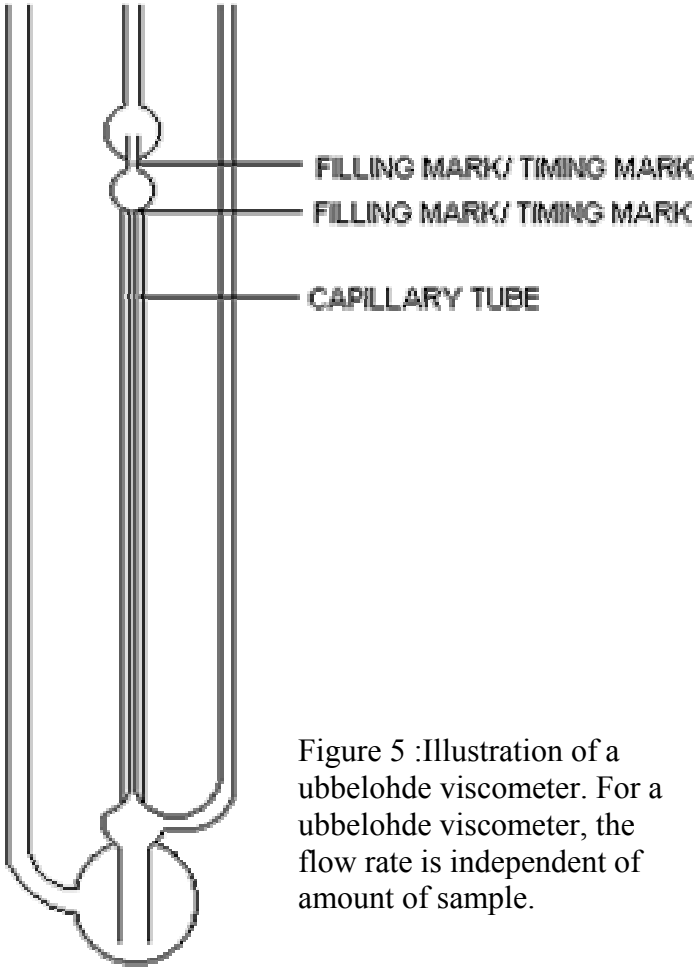

Figure 5 :Illustration of a ubbelohde viscometer. For a ubbelohde viscometer, the flow rate is independent of amount of sample.

Poiseuilles law for flow rate (eq. 6) is valid for fluids that possess Newtonian flow.

6) $dV/dt = \pi R^4 \rho gL/8\eta L)$

In equation 6, dV/dt is the volume flow rate, ρgL is the pressure difference driving the flow, η is the viscosity of the fluid, and R is the radius of the capillary through which the fluid flows.
Neglecting end effects of the capillary and slip between the capillary wall and the solution, the volume flow rate
dV/dt=V/t is constant over the capillary. The viscosity of a solution η_1 relative to the solvent η_0 can be expressed by (eq. 7):

7) $\eta_1 = \eta_0 \cdot (\rho_1 \cdot t_1) / (\rho_0 \cdot t_0)$

In equation 7, subscripts "0" and "1" relates to solvent and solution, respectively, and t is time of flow.

The reduced viscosity η_{red} of a solution with polymer concentration c is:

8) $\eta_{red} = (\eta_1 - \eta_0) / \eta_0 \cdot c$

By assuming that $\rho_1 \approx \rho_2$, equation 6, 7 and 8 gives (eq. 9):

9) $\eta_{red} = (t_1 - t_0) / (t_0 \cdot c)$

3.4.2 Huggins equation[42]

The Einstein-Guth equation (eq. 10) describes the viscosity η_1 of dispersions of small spherical particles of volume fraction φ_2 in a solvent with viscosity η_0:

10) $\eta_1 = \eta_0 \cdot (1 + B_1\varphi_2 + B_2\varphi_2^2 + \ldots..)$

In equation 10, B_1 and B_2 are coefficients, which depends on the form on the solvated particles. For rigid spheres, $B_1=5/2$. The equation applies to polymer in a solvent in the dilute regime, when the polymer molecules exist as individual coils.

Intrinsic viscosity $[\eta]$ (eq. 11) is the reduced viscosity (eq. 8) of a solution at infinite dilution ($c \rightarrow 0$):

11) $[\eta] = \lim_{c \rightarrow 0} (\eta_1 - \eta_0)/(\eta_0 \cdot c)$

With equation 10 and 11 and $\varphi_2 = c \cdot V_h N_A / M$, $[\eta]$ becomes (eq.12):

12) $[\eta] = \lim_{c \rightarrow 0} (B_1 V_h N_A / M + B_2 (V_h N_A / M)^2 c + \ldots..) = B_1 \cdot (V_h N_A / M)$

N_A, M and c is Avogadros number, molar mass and the mass concentration of the polymer molecules. V_h is hydrodynamic volume of free draining polymer coils, when there are no hydrodynamic interactions between the coil segments. With $V_h = M/\rho \cdot N_A$, where ρ is density of the polymer coil, $[\eta]$ becomes:

13) $[\eta] = 5/(2 \cdot \rho)$

$[\eta]$ is the specific volume of polymer coils at infinite dilution. Overlap concentration c* is the concentration of polymer when the polymer coils start to overlap in solution and the volume fraction of polymer[1] $\varphi_2 = c/\rho \approx 0{,}4$. The relation between c* and $[\eta]$ is (eq. 14):

14) $[\eta] \approx 1/c^*$

An expression for η_{red} for a polymer solution can be derived from equation 10 and 13:

15) $\eta_{red} = [\eta] + (B_2/B_1^2)\cdot[\eta]^2c+\ldots$

The coefficient (B_2/B_1^2) is termed Huggins constant (k_H). Equation 16 is Huggins equation:

16) $\eta_{red} = [\eta] + k_H [\eta]^2c+\ldots.$

With the estimated expression for reduced viscosity (eq. 9), $[\eta]$ and k_H can be obtained from time-measurements in capillary viscosimetry (eq. 17).

17) $(t_1- t_0)/ t_0c = [\eta] + k_H [\eta]^2c +\ldots.$

In dilute systems of polymer, the hydrodynamic interactions are determining the size of the polymer coils in the solution. Kirkwood-Riseman-theory describes variable hydrodynamic interactions. When the hydrodynamic interactions are strong, the coils are contracted, and the solvent is impeded from flowing through the coils, which leads to less friction between solvent and the polymer segments and hence to a lower solution viscosity. At weaker hydrodynamic interactions, the coils are more extended, the flow of solvent through the coil is increased, which increases the friction between solvent and polymer and the solution viscosity increases[42].

3.5 Shear viscosity

In shear viscosity measurements, the apparent viscosity η is measured at different strains, to give η as a function of the rate of strain $d\gamma/dt$. In shear viscosity measurements with the cone plate geometry, the shear rate $(d\gamma/dt)$ is constant in the sample due to the small angle between the cone and the plate[42]. The cone-plate device is appropriate for measurements on viscous solutions and gels[43]. In shear viscosity measurements with the cone-plate-device, the sample is added between the cone and the plate, and shear strain is applied to the sample through a displacement in the cone. The sample give a stress response, which is registrated by measuring head as a torque M. M and the velocity n of the deformation are sizes from the measuring system, which are converted to strain rate $d\gamma/dt$ and stress σ by the PC connected to the rheometer. The converting equations are:

18) $\sigma= \sigma_{‰}\cdot M_{‰}$

19) $d\gamma/dt = k\cdot n$

In equation 18 and 19, σ‰ and k are constants depending on the geometry of measurements used. A schematic representation of the rheometer with cone-plate-geometry is shown in figure 6.

In the figure, the angle between the cone
and the plate is enlarged. For ideal, Newtonian liquids, the viscosity η in the sample is constant in increasing $(d\gamma/dt)$, and the stress σ in the sample is proportional to $(d\gamma/dt)$. Viscoelastic systems have both fluid and elastic mechanical properties1. The (apparent) viscosity of such systems is given

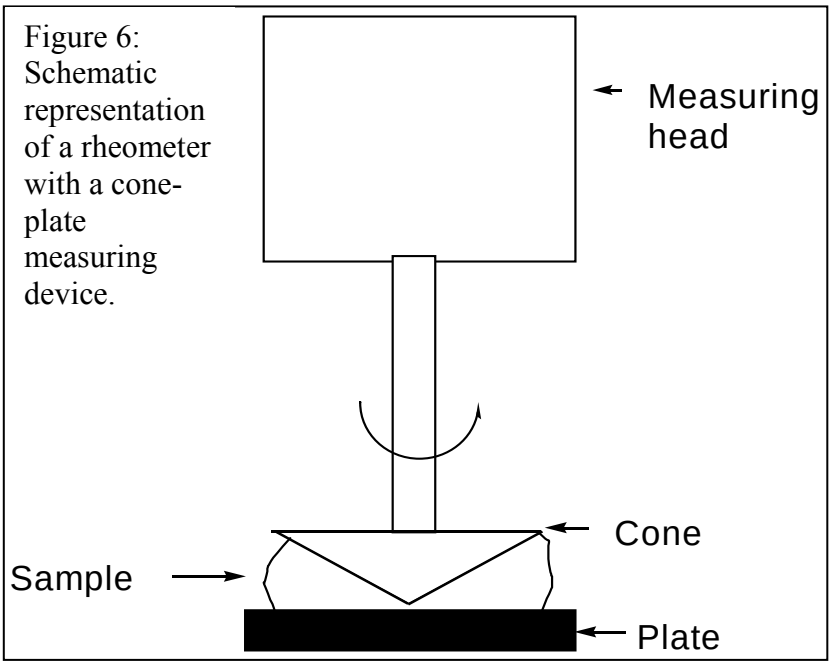

Figure 6: Schematic representation of a rheometer with a cone-plate measuring device.

as the ratio between the stress in the solution and the applied shear rate (eq. 20)

$$20)\ \eta = \sigma/(d\gamma/dt)$$

Many viscoelastic fluids show shear thinning behaviour. When a shear is applied to a viscoelastic solution, the shear viscosity is constant at low ($d\gamma/dt$), but decreases at higher ($d\gamma/dt$). The region with constant η in the start of the curve is termed the Newtonian plateau, and η in this region is termed zero shear viscosity, η_0, defined in eq. 21:

$$21)\ \eta_0 = \lim_{d\gamma/dt \to 0} \eta$$

The onset of decrease in η occur at a critical shear rate, $(d\gamma/dt)_c$. The following region with a decrease in η is termed the shear thinning region. Shear thinning behaviour appears for entangled systems of polymer[1] and in associating -polymer systems, for example in systems of solutions of hydrophobically modified polymer, and in systems of interaction between HM-polymer and surfactant[15]. In the above systems, the network is physical, which has reversible junctions that can break under applied shear and hence show shear thinning[1]. The shear viscosity profile for a shear thinning, pseudoplastic[44] materials follow the Cross-model[43] (eq. 22):

$$22)\ (\eta_0-\eta)/(\eta-\eta_\infty) = K(d\gamma/dt)^m$$

η_0 is the zero shear viscosity, η_∞ is the viscosity at high, η is the solution viscosity, $d\gamma/dt$ is the shear rate and K and m are constants. When $\eta_0 >> \eta >> \eta_\infty$, equation 22 reduces to:

$$23)\ \eta = K\,(d\gamma/dt)^{n-1}$$

When $n<1$, the fluid is shear thinning. For $n = 1$, the fluid is Newtonian, and η is constant.

The critical shear rate $(d\gamma/dt)_c$ which marks the onset of shear thinning is approximately the same as the cross-over frequency ω_c where $G'(\omega_c) = G''(\omega_c)$ from oscillatory shear measurements. The characteristic relaxation time τ^* of the solution is approximately:

24) $\tau^* \approx 1/(d\gamma/dt)_c$

The characteristic relaxation time is approximately the longest time for the elastic structures in the solution to relax[1].

4 METHODS

4.1 Synthesis of HMHEC

4.1.1 Materials and purification

The materials (table 1) were HEC (Natrosol250 GR LOT 0403,Aqualon/Hercules), NaOH (MERCK, 98,0-100,5%), bromo-tetradecane (Fluka, purum≥97% (GC)), dimethylacetamide (DMA, Riedel-de Haën, min 99% (GC)). Acetone, (Sceda Chemie, min 95,5% pure) was used in the purification of the product.

HEC was purified as follows: HEC was dissolved in ionic-changed water to a concentration of 1,5 w/w% by swelling while stirring with a magnetic stirrer at room temperature. The solution was then centrifuged for 3 hours at 2000 r.p.min. to remove high molecular HEC and impurities.

Secondly, the HEC- solution was dialysed against distilled water for 3-4 days, and against double-distilled water for another 3-4 days. Smaller impurities, such as salts, were removed in this step. The dialysis was stopped when the conductivity of the expelled water showed values below 1-2 mS/cm.

Third, the HEC- solution was freeze-dried for 3 days to remove water from the polymer, and the dried HEC stored on plastic-bottles in desiccator.

4.1.2 Synthesis

HEC was added to DMA, and the polymer was allowed to swell in the solvent for three days. NaOH dissolved in water (see table 2) was added slowly and dropwise to the homogeneous mixture during stirring. The mixture was continuously degassed by nitrogen gas to prevent oxidation of the polymer from the air-O_2. Polymer (white) precipitated during the addition of NaOH. The precipitate was possibly ionic HEC-NaOH- activate, which precipitated from the nonpolar solvent. The precipitate was formed by oxidation of hydroxy-groups on HEC by NaOH, described in equation A[45] below.

A. $R_{cell}O(CH_2CH_2O)_nH + NaOH \rightarrow R_{cell}O(CH_2CH_2O)_{n-1}CH_2CH_2O^- + Na^+ + H_2O$

In equation A, the ionic polymer-activate is termed $R_{cell}O(CH_2CH_2O)_{n-1}CH_2CH_2O^-$, where R_{cell} terms the cellulose backbone of HEC, which is substituted with n ethylene oxide groups per repeating unit of the polymer. The temperature on the oil bath was set to 80 °C, and

bromotetradecane, (see table 2) diluted by 20 ml DMA, was added dropwise during 40 min. to the reaction medium during stirring. The [HEC] was now 1,8w/w%. During the addition of bromotetradecane, the precipitate (eq. A) slowly dissolved. This was possibly due to reaction of the bromotetradecane with the ionic O^- sites on the HEC-NaOH-activate (eq. B)[45], which is the final step in the hydrophobically modification process of HEC to HMHEC.

B. $R_{cell}O(CH_2CH_2O)_{n-1}CH_2CH_2O^- + Br(CH_2)_{12}CH_3 \rightarrow R_{cell}O(CH_2CH_2O)_n\ (CH_2)_{12}CH_3 + Br^-$

The reaction was stopped after 40h and 40min.by precipitating of the polymer in 6 L acetone. The polymer was then filtrated, and washed with acetone. The polymer was dissolved in 600 ml DMA, and precipitated in 8 L acetone two times, to remove unreacted alkyl halide. Then the polymer was stored in a vacuum oven at 30 °C for 2 days to remove acetone.

Next, the polymer was dissolved in water to a concentration of 1w/w % and left stand for 1 day to let the polymer swell. The solution was stirred but still after long time of stirring, the solution was turbid. Next, the solution was centrifuged at 2000 rpm for 3 hours to separate the water soluble polymer from the precipitate.

That some of the polymer did not dissolve in water can possibly be due to a high hydrophobicity on certain places on the polymer, as a result of an inhomogeneous reaction. The critical step in the reaction was the formation of the HEC-NaOH-activate, which determined the reaction sites on the polymer for the reaction with alkylbromide. Addition of the NaOH-solution in to large droplets or in a too short time-interval accompanied by poor stirring mechanism can have resulted in an uneven distribution of reaction sites for the alkylbromide, and to local places on the polymer with a high degree of hydrophobically modification.

The HMHEC precipitate was freeze dried in order to remove rests of solvent (water and acetone), and analysed by ^1H NMR. In the further text, this HMHEC is termed HMHEC 2.

4.2 Synthesis of hexanediyl-1,6-bis(dimethyldodecylammonium bromide) (12-6-12)

4.2.1 Materials

The reagents for the synthesis were 1,6-dibromohexane (Aldrich, 96% pure) and N,N-dimethyldodecylamine (Aldrich, 97% pure). Acetone (Sceda Chemie, min 95,5% pure), chloroform (Prolabo, 99-99,6% pure).
All reagents were used as received.

Amounts of reactants are in table 2 in appendix.

4.2.2 Synthesis[21]

The reaction equation for the synthesis of 12-6-12 is given in equation C below.

C. Br(CH2)6Br (l) + 2 N(CH2)11CH3 (l) → (CH2)6(N+(CH2)11CH3)2 (s) + 2Br-

The synthesis was performed twice, termed synthesis 1a) and 1b).

A round-bottom flask was oven dried at 200°C for 18 hours, then acetone (50 ml, 1a), 500ml, 1b)) was added to the flask and heated carefully with stirring until boiling (app. 56°C) Then 1,6-dibromohexane was added to the flask. Next, N,N-dimethyldodecylamine in excess, dissolved in acetone (3ml, 1a), 30ml, 1b)) was added to the flask. The reacting system was stirred at room-temperature for about 2 h, until a white precipitate was formed. More acetone (25ml, 1a), 250ml, 1b)) was added to the system. The reaction was continued for about 40 hours, and the product, a white, fine-crystalline powder, was filtered trough a Büchner funnel trough a double-layer of 589-3 filter paper.

The product was then recrystallized three times with a mixture of chloroform and acetone in the ratio 1:4. Thereafter, the product was dried in vacuum-oven at 60°C, to remove contents of acetone and chloroform.

4.3 Synthesis of dimethylparaphenyl-α,ω-bis(dimethyldodecylammonium bromide) (12-φ-12)

4.3.1 Materials

The reagents for the synthesis were p-di(bromomethyl)benzene (Fluka, ≥98% pure), and N,N-dimethyldodecylamine (Aldrich, 97% pure). Acetone (Sceda Chemie, min 95,5% pure), chloroform (Prolabo, 99-99,6% pure) All reagents were used as received.

Amounts of reactants are in table 2 in appendix.

4.3.2 Synthesis[21]

The reaction equation for formation of 12-φ-12 is given in equation D below.

D. $Br(CH2)Ph(CH2)Br\ (l) + 2\ N(CH2)11CH3\ (l) \rightarrow$

$(CH2Ph\ CH2)(N+(CH2)11CH3)2\ (s) + 2Br-$

The synthesis was performed twice, termed synthesis 2a) and 2b).

Acetone (13 ml, 2a), 500ml, 2b)) was added to a round-bottom flask and heated carefully with stirring until boiling (app. 56°C). Then p-di(bromomethyl)benzene was added to the flask. Next, N,N-dimethyldodecylamine in excess, dissolved in acetone (1 ml, 2a), 30ml, 2b)) was added to the flask, and a white precipitate formed immediately. The reacting system was stirred at room temperature for about 20h. The product, a white, fine-crystalline powder, was filtered trough a Büchner funnel trough a double-layer of 589-3 filter paper .

The less chloroform-soluble product was then recrystallized three times with a mixture of chloroform and acetone in the ratio 1:2. Thereafter, the product was dried in vacuum-oven at 60°C, to remove contents of acetone and chloroform.

4.4 Capillary viscosimetry

4.4.1 Materials and sample preparation

The materials were HMHEC (Natrosol Plus 331 LOT V-1302, purification, see 4.1.1), HMHEC 2 (synthesis/purification, see 4.1.2.), DoTAB (Fluka, puriss pa. ≥99% (AT), used as received), hexanediyl-1,6-bis(dimethyldodecylammonium bromide) (12-6-12) (synthesis/purification, see 4.2.2.), filters (MFS, CA-membrane, 0,8μm pore)

The DoTAB and 12-6-12 solutions were prepared by dissolving the weighed compound in the weighed amount of double distilled water.

Stock solutions of HMHEC were made by dissolving HMHEC in a weighed amount of solvent (water/water+DoTAB/water+12-6-12). The HMHEC stock solutions were swelled and equilibrated for a day at room temperature. Thereafter the solutions were stirred with a magnetic stirrer for a day to make the solution homogeneous. Samples of HMHEC 2/water, HMHEC/water and HMHEC/DoTAB/water and HMHEC/12-6-12-/water were prepared. The samples were prepared by diluting the stock solution with the same solvent as for the stock solution. Each series consisted of 5-6 samples of different HMHEC-concentration. After dilution, the samples were stirred for 1 day to make them homogeneous.

4.4.2 Measurements

The viscosity measurements (table 7) were performed with an Ubbelohde viscometer dipped in a thermostated water bath at 25°C . The temperature was collected before each measurement, and the mean value and standard deviation in temperature for the repeating measurements on a solution is in table 8. The solutions were thermostated in minimum 15 min in the bath before each measurement.

Between each new sample, the viscometer was rinsed by flushing with distilled water, filled with 68wt% HNO_3, and let it stand for at least 1/2 hour. The acid was poured out and the viscometer was filled and shaken with some chrome –sulphuric acid to remove rests of polymer solution. Least, it was flushed several times with water to remove rests of acid. The pH of the expelled water was checked out with pH-paper, and compared with pH of distilled water. Between each new sample, the flow time was measured for distilled water as a reference. There was some variance in the flow time of distilled water, possibly due to changes in the composition of the glass wall of the viscometer, due to the strong acid. This touches the reproducibility of the measurements; the variation in the reference-time measured for water increases the uncertainty in the measurements and the calculations of reduced viscosity η_{red}, and in the values of intrinsic viscosity and Huggins constant, derived from η_{red}. A systematic error in η_{red} is due to the difference in surfactant concentration in the reference-solution with surfactant and the sample solution of surfactant and HMHEC. The error becomes larger the more surfactant is adsorbed to HMHEC, especially in the co-operative region of the adsorption, around CMC of the surfactant. This error could have been corrected for by measuring of the actual concentration of free surfactant in the sample solution by a surfactant-sensitive-electrode, which was not performed in this work. This leads to large uncertainties in the values of η_{red}, and in larger degree for the derived values of intrinsic viscosity $[\eta]$ and Huggins constant k_H. The curves of $[\eta]$ and k_H plotted against concentration of surfactant merely show a tendency than true values of the parameters.

Prior to each measurement, 5ml sample was flushed through the viscometer, to minimalize concentration errors. The sample solution (12ml) was added to the viscometer through a syringe. Samples were filtrated before adding the solution to the viscometer, to remove dust particles from the sample. Bubbles of air in the sample were removed with a syringe before each measurement. The solution was risen through the capillary with a pump to a position above the upper marking, and the time needed for the meniscus of the solution to pass between the two markings on the viscometer was measured. The time was measured with a stop-watch, giving an accuracy of 0,01 s. The measurement was repeated 5-7 times on each solution depending on the variation in the measurements. The temperature was read off before and after each measurement, with an accuracy of two decimals. The variation in temperature was max. 0,03 K.

For some of the solutions of 1,5 mmolal 12-6-12/HMHEC, it became almost impossible to force the solution through the filters. In measuring on a filtrated solution and an unfiltrated sample, the flow time was ca. 3s longer for the unfiltrated than for the filtrated sample, possibly due to that polymer had adsorbed to the filter, giving a lower concentration of the sample. Therefore, measurements on the solutions with 1,5mmolal 12-6-12 and 0,07 , 0,09 , and 0,11g/dl HMHEC was run without filtration of the solution. For the HMHEC solutions with 0,2 , 1,2 , 3 and 6 mmolal 12-6-12 and 3 , 10 and 18 mmolal DoTAB, the solutions were not filtrated prior to measurement.
This caused some dust particles in the viscometer for the unfiltrated samples.

4.5 Shear viscosity

4.5.1 Materials and sample preparation

The materials were HMHEC (Natrosol Plus 331 LOT V-1302, purification, see 4.1.1), termed HMHEC , DoTAB (Fluka, puriss pa. ≥99% (AT), used as received) and hexanediyl-1,6-bis(dimethyldodecylammonium bromide) (12-6-12) (synthesis/purification, see 4.2.2.)

Samples of HMHEC/water and HMHEC/DoTAB/water and HMHEC/12-6-12-/water were prepared. (table 3 and 4 in appendix)
Solutions of DoTAB and 12-6-12 were prepared by dissolving a weighed amount of surfactant in a weighed amount of double distilled water.
The samples were prepared by weighing out equal amount of HMHEC into each bottle, then 10 g of the respective solution (DoTAB+water/12-6-12+water / water) was added to each bottle. The bottles were capped and wrapped in Parafilm, to keep the correct concentration. The solutions were equilibrated and swelled for 2 days in room temperature, to make the solutions swell, thereafter they were stirred at room temperature for 1 day to make the solutions homogeneous.

4.5.2 Measurements

The flow curves were obtained for the samples by measuring shear viscosity at different shear rates (table 13 and 14). The rate of shear was in the range 0,01-1000 s^{-1}. The measurements were performed with the cone-plate-geometry with a plate radius of 7,5 cm and a cone angle of 1° (CP 75-1).The measurements were carried out with a Modular Compact rheometer from Physica, with a MCR300 measuring device. As software, Universal Software US 200 was used. The measuring temperature was 25°C, and the sample and the sample cell was heated with a peltier-element.

Prior to measurements, the instrument was initialised by checking the vertical reference point and the reference angle of the measuring drive system. The electronics in the instrument were warmed up to reach operating temperature for 1 hour before the measurements started. Then the measuring system (CP 75-1) was installed, and the normal force on the plate and the motor (20 min, to compensate for the air bearing friction) were adjusted. The zero-gap of the cone and plate was set. The sample was then placed on the plate gently with a capped tube, to disturb the sample as less as possible. A metal ring enclosed the sample, and a lid was placed over the sample and the cone. The gap between plane and cone was filled with silicone oil, to prevent evaporation of the solvent. The rheometer was kept in an outer glass cage, in order to prevent disturbances in the air around the sample. The temperature was set, and the system was equilibrated in 20 min. to ensure correct temperature.

A shear strain rate $d\gamma/dt$ was applied to the sample through the cone, which gave a stress response σ from the sample, registrated by the measuring head as a torque M. The measurement was repeated for several shear rates $d\gamma/dt$ for each sample. The shear rate $d\gamma/dt$ was calculated from the applied velocity n, and the stress response in the sample was calculated from the torque M by the software through eq. 18 and 19. The constants $\sigma_{‰}$ and k for the CP75-1 geometry is $\sigma_{‰} = 0{,}453$ Pa, and $k = 6{,}000\ s^{-1}$ (adapted from instruction manual of the rheometer used). The small cone angle of 1° ensured a constant shear rate through the sample.

4.6 ^{1}H NMR

4.6.1 Materials

Solvents used for the ^{1}H NMR samples were: D_2O (Apollo, 99,92 atom% D) for the HEC sample ,$CDCl_3$ (Cortec, 99,8 atom% D) for the samples of hexanediyl-1,6-bis(dimethyldodecylammonium bromide) (12-6-12) and dimethylparaphenyl-α,ω-bis(dimethyldodecylammonium bromide) (12-φ-12) and DMF-d_7 (Cambridge Isotope Laboratories, Inc./CIL, 99% D) for the HMHEC 2 sample. NMR- tubes (AMEX, MINIPUL, NORELL, Inc. prescored, i.d.: 4,2 m m, o.d.:4,97m m.).

4.6.2 Sample preparation

Samples of 12-6-12 and 12-φ-12 were prepared by dissolving the compound in $CDCl_3$ directly in the NMR-tube. The samples of HMHEC 2 and HEC were prepared by weighing out polymer and D_2O in the tube, then the tubes were stored in a cold place, to let the solutions swell. The tubes were capped to prevent evaporation of the solvent, and at least the solutions were stirred carefully, to make them homogeneous. An overwiev of the NMR-samples is given in table 3 in appendix.

4.6.3 Measurements

The ^{1}H NMR -measurements were carried out at room temperature.
The NMR measurements were carried out with a Bruker Spectrospin Avance DPX 200 MHz ^{1}H NMR spectrometer, with 5mm probes.
The instrument was connected to a 52 M M magnet (Bruker and Spectrospin).

An “Indy” computer operated the spectrometer. The software was IRIX 6.5.6 with the Bruker acquisition and processing software package Xwinnmr 2.6.
The magnet is cooled by liquid He.

4.7 Mass spectrometry

4.7.1 Sample preparation

The compounds hexanediyl-1,6-bis(dimethyldodecylammonium bromide) (12-6-12) (synthesis/purification see 4.2.2.) and dimethylparaphenyl-α,ω-bis(dimethyldodecylammonium bromide) (12-φ-12) (synthesis/purification see 4.3.2.) were dissolved in double distilled water prior to analysis.

4.7.2 Measurements

The measurements were carried out on a QTOF (Quadrupole Time Of Flight) 2W, Prospec Q-mass spectrometer from Micromass. The samples were injected into the mass spectrometer by “direct probe”-method by a infusion pump.The ionisation method used was “Electrospray positive ions” (ESI). A ”time-of-flight” (TOF) mass separator was used (3.3).

The spectrometer was cleaned prior to the measurement by removing rests of complexating methanoic acide and by running a blind test (water).

4.8 Melting point determinations

4.8.1 Materials and sample preparation

The samples of hexanediyl-1,6-bis(dimethyldodecylammonium bromide) (12-6-12) (synthesis/purification see 4.2.2.) and dimethylparaphenyl-α,ω-bis(dimethyldodecylammonium bromide) (12-φ-12) (synthesis/purification see 4.3.2.) were prepared in thin glass-capillary tubes, closed in one end.

4.8.2 Measurements

The melting point of 12-6-12 and 12-φ-12 (table 4) was determined with a Büchi 530 instrument. The capillary tubes were dipped into a glycerol bath and were observed through an enlarging glass window. The sample was then heated carefully. The temperature was read off manually from a fine-graded thermometer. The melting point was read off as an interval, the first temperature reading in the start of the melting, and the second read-off was when the sample was completely melted.

The melting point was measured in two repetitions.

5 RESULTS AND DISCUSSION

5.1 HMHEC 2

5.1.1 ^{1}H NMR

The ^{1}H NMR-spectra in figure 8 and 9 are for HEC, and the ^{1}H NMR-spectra in figure 10 and 11 are for HMHEC 2. A structure of the repeating units of HEC and HMHEC is shown in figure 7.

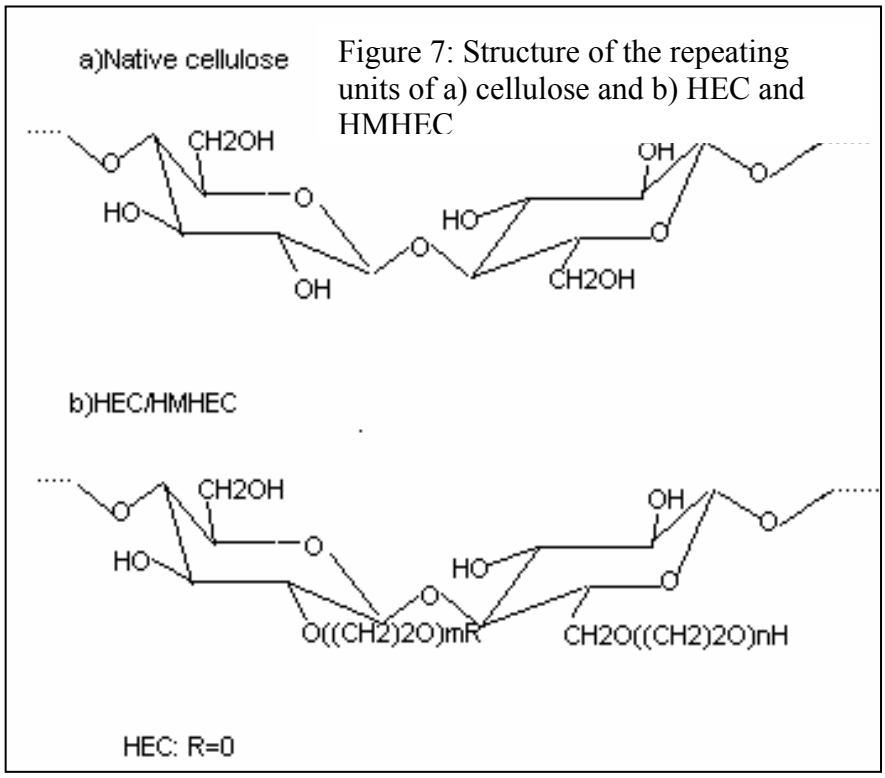

Figure 7: Structure of the repeating units of a) cellulose and b) HEC and HMHEC

The spectra of HEC and HMHEC 2 in figure 8 and 10 both show a main peak between 4,25-2,5 ppm which possibly is due to the HEC backbone since it appears for both polymers. The peak is shifted to high ppm values typical for protons bound to O-atoms[39] (ppm 3-4,5) and for protons bound to C-atoms near O-atoms. The peaks in the interval 3-1,5 ppm in figure 10 is due to dimethyl formamide[38] (DMF, δ=2,744, δ=2,915 and

δ=8,022) from the solvent. Figure 11 show to smaller peaks in the region 1,4-0,75ppm, which are absent on the enlarged diagram of HEC in figure 9, and the peaks are possibly due to the hydrophobic groups (tetradecane-chains) of HMHEC 2. The two peaks are shifted to low ppm- values 1,65-1,0ppm and 1,0-0,75ppm. The peak in the first interval is typical for C-CH_2 –protons[40], and is possible due to protons on the tetradecane chains on the HEC-backbone not attached to the carbons adjacent the oxygen in the ring. The shift of the second peak in figure 11 is typical for C-CH_3 protons[40]. It is shifted further down, typical for the longer distance to the O-atoms on the ring, and could be due to the protons on the terminal methylene groups on the alkyl chains.

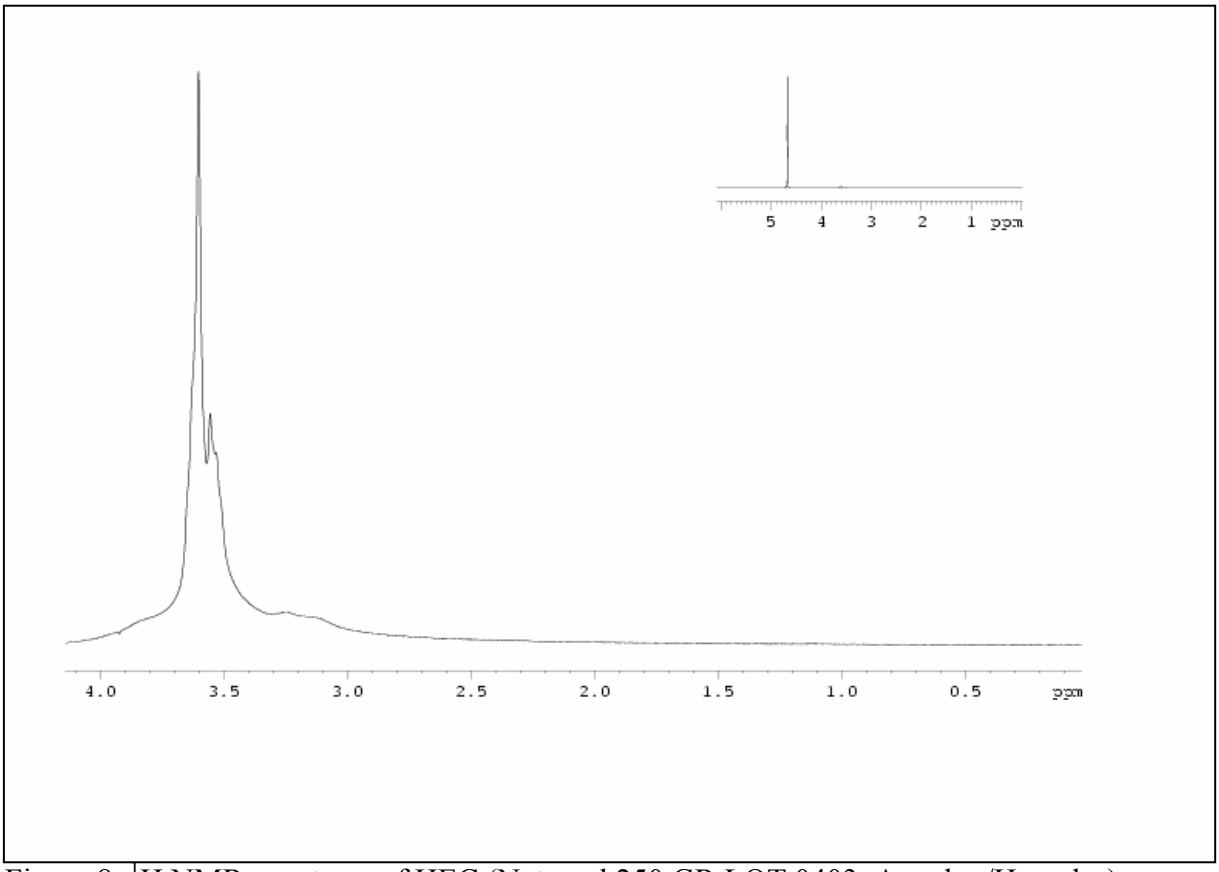

Figure 8: ^{1}H NMR-spectrum of HEC (Natrosol 250 GR LOT 0403, Aqualon/Hercules)

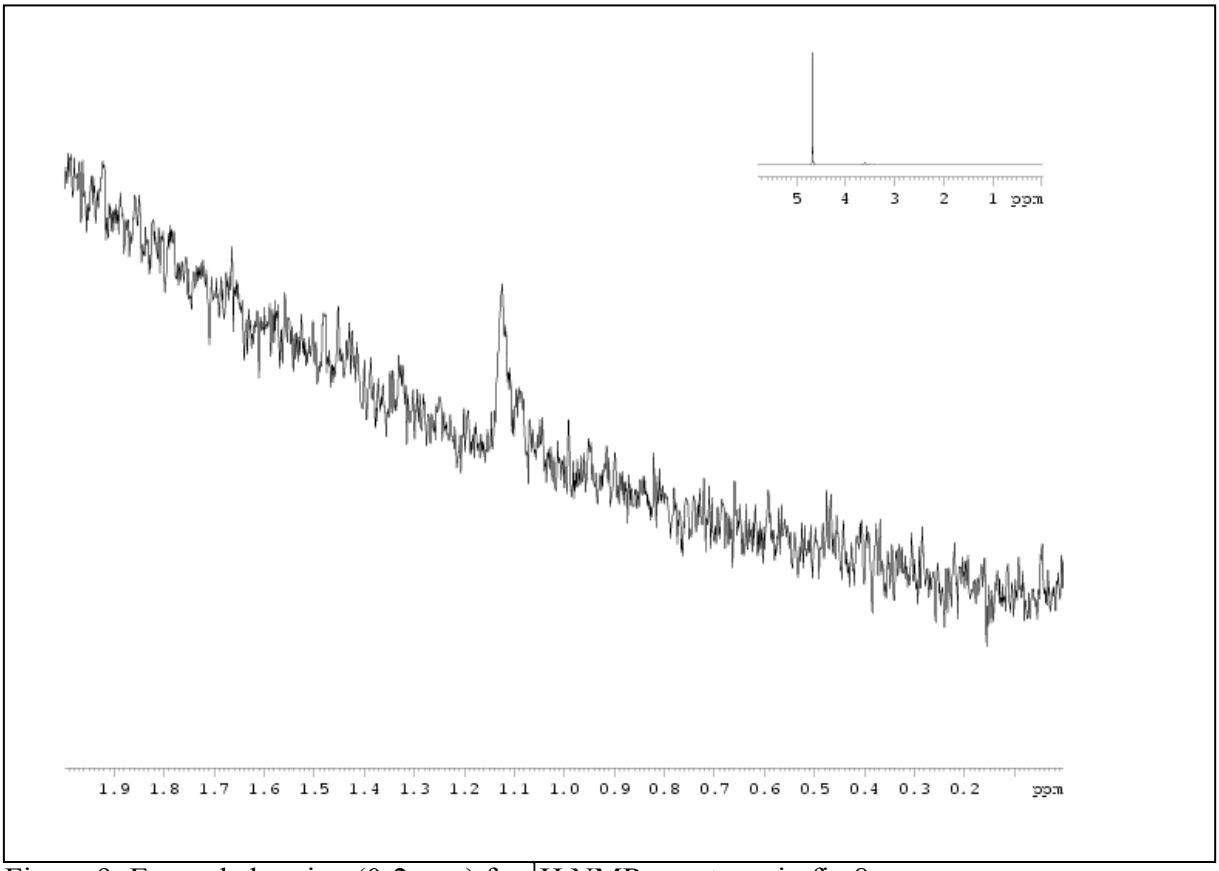

Figure 9: Expanded region (0-2ppm) for ^{1}H NMR spectrum in fig.8.

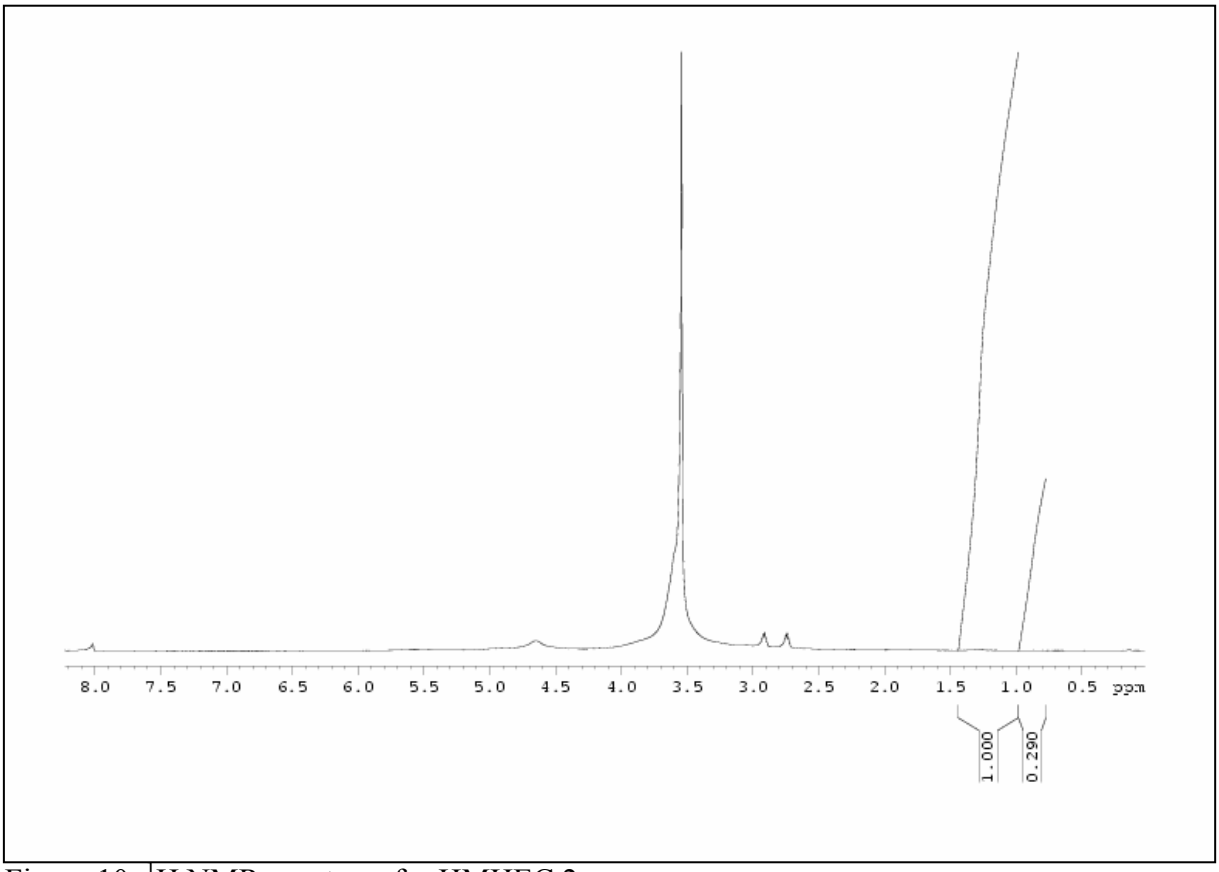

Figure 10: ^{1}H NMR spectrum for HMHEC 2.

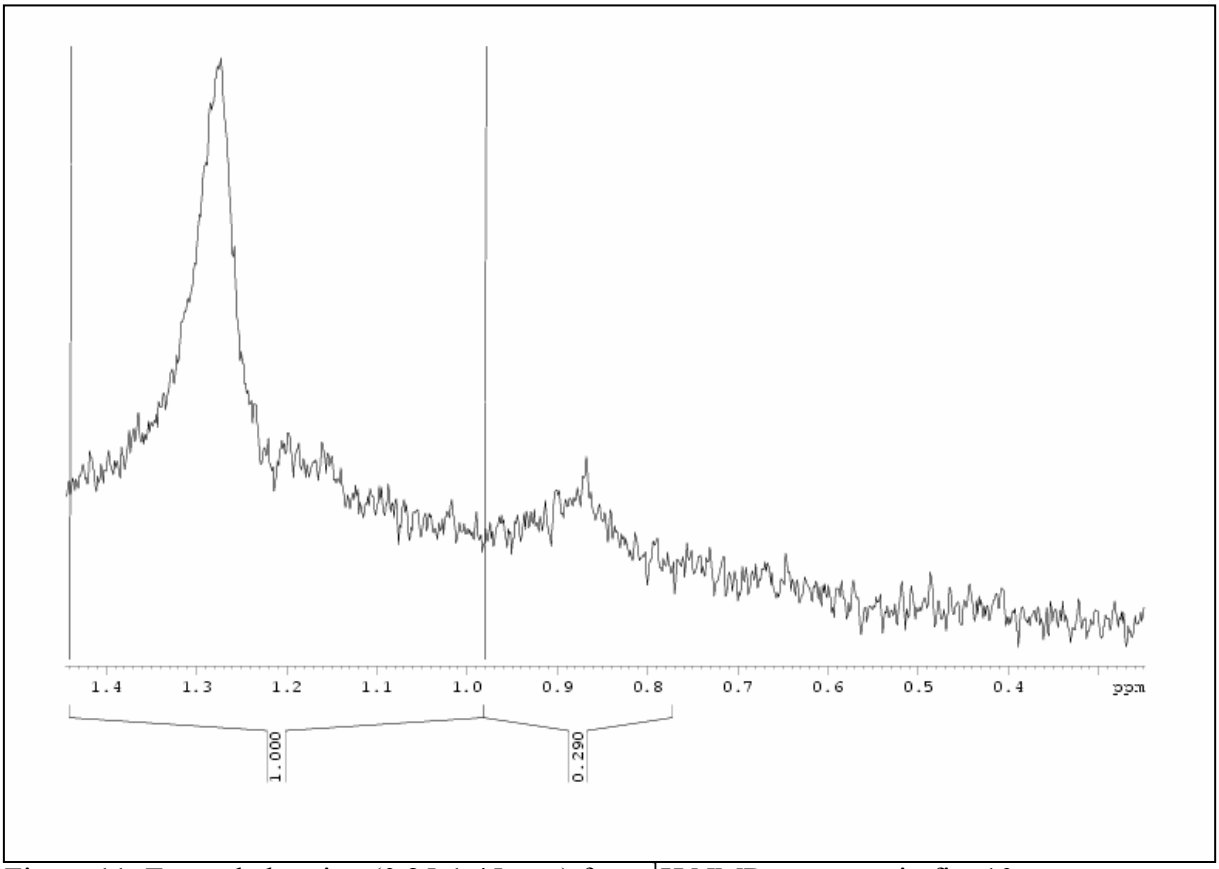

Figure 11: Expanded region (0,25-1.45ppm) from ^{1}H NMR spectrum in fig. 10

5.2 Gemini surfactants

5.2.1 ^{1}H NMR

5.2.1.1 hexanediyl-1,6-bis(dimethyldodecylammonium bromide) (12-6-12)

Figure 12 show a ^{1}H NMR spectrum for the synthesised 12-6-12. The structure of 12-6-12 is given in figure 13.

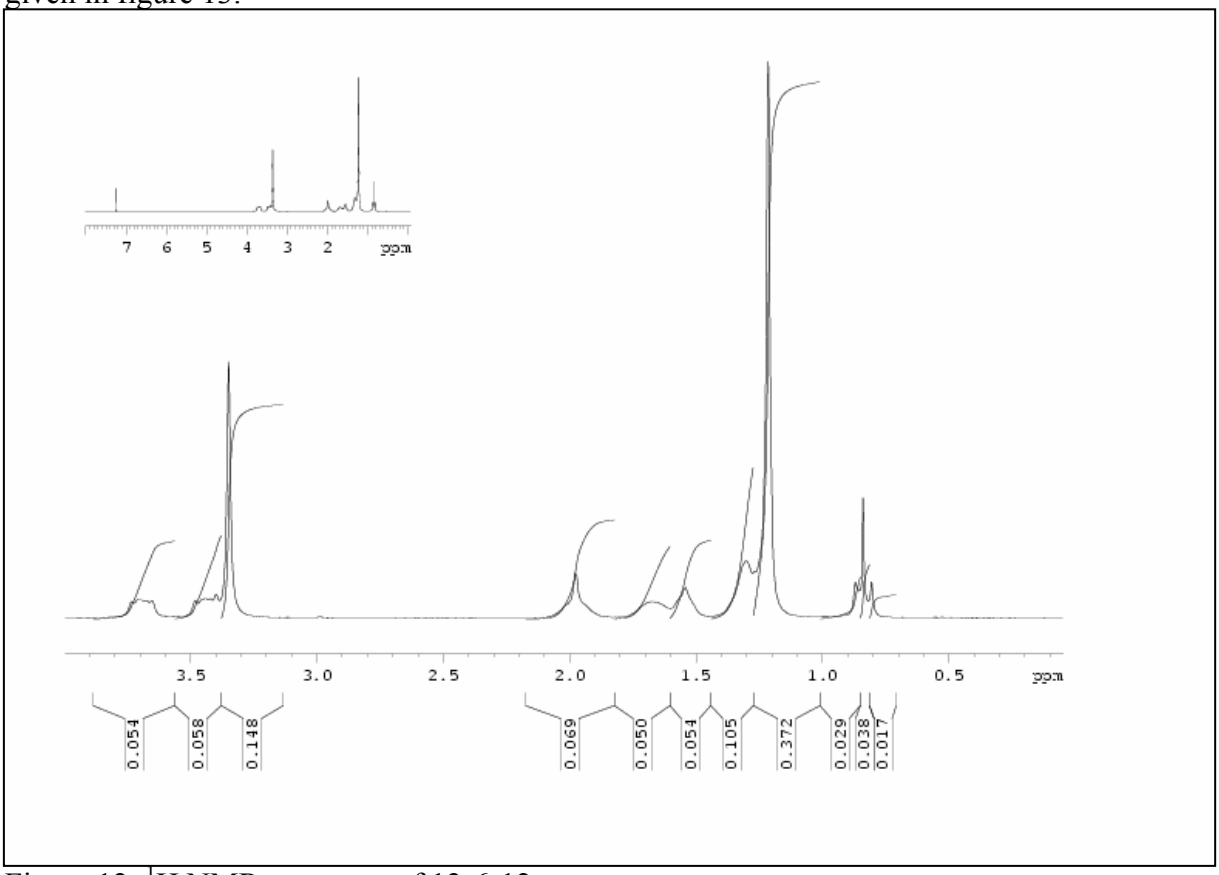

Figure 12: ^{1}H NMR-spectrum of 12-6-12.

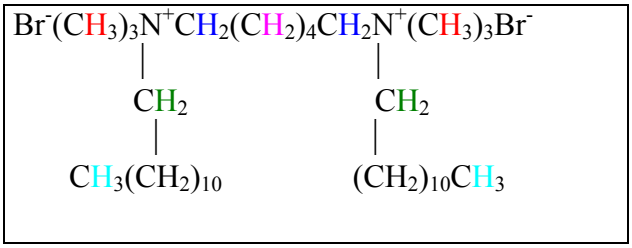

Figure 13: Structure of 12-6-12.

The highest shifted peak in the diagram, at 7,258 ppm, is due to chloroform[38] in the sample solvent. –CH-N-protons[40] have a shift of 2,2-2,9 ppm. The positive charge on the N-atom in 12-6-12 make the shift values higher, the three peaks in the interval 3,9-3,2 ppm possibly corresponds to protons attached to C-atoms bound to the N-atoms: The first peak is due to H on C bound to N in the spacer group (blue, fig.13), the second peak is H from C bound to N in the long hydrocarbon-chains (green, fig.13), and the third peak corresponds to H in the methylene-groups on N (red, fig.13). The latter is a singlet, corresponding to no coupling

protons bound to N. The fourth peak (δ = 2,051 ppm)[38] is possible due to acetone. Protons in the spacer group are nearest to the N-atoms and are shifted higher in the spectrum than protons in the tails. Peak 5 and 6 are due to protons in the spacer group (pink, fig.13), and peaks 7 and 8 are due to protons in the tails (black, fig.13), The last peak corresponds to the methylene protons on the end of the tails (cyan, fig.13). The integrals are listed in table 5 in appendix..

5.2.1.2. dimethylparaphenyl-α,ω-bis(dimethyldodecylammonium bromide) (12-φ-12)

Figure 14 show a ^{1}H NMR-spectrum of 12-φ-12. A simple structure of 12-φ-12 is given i figure 15.

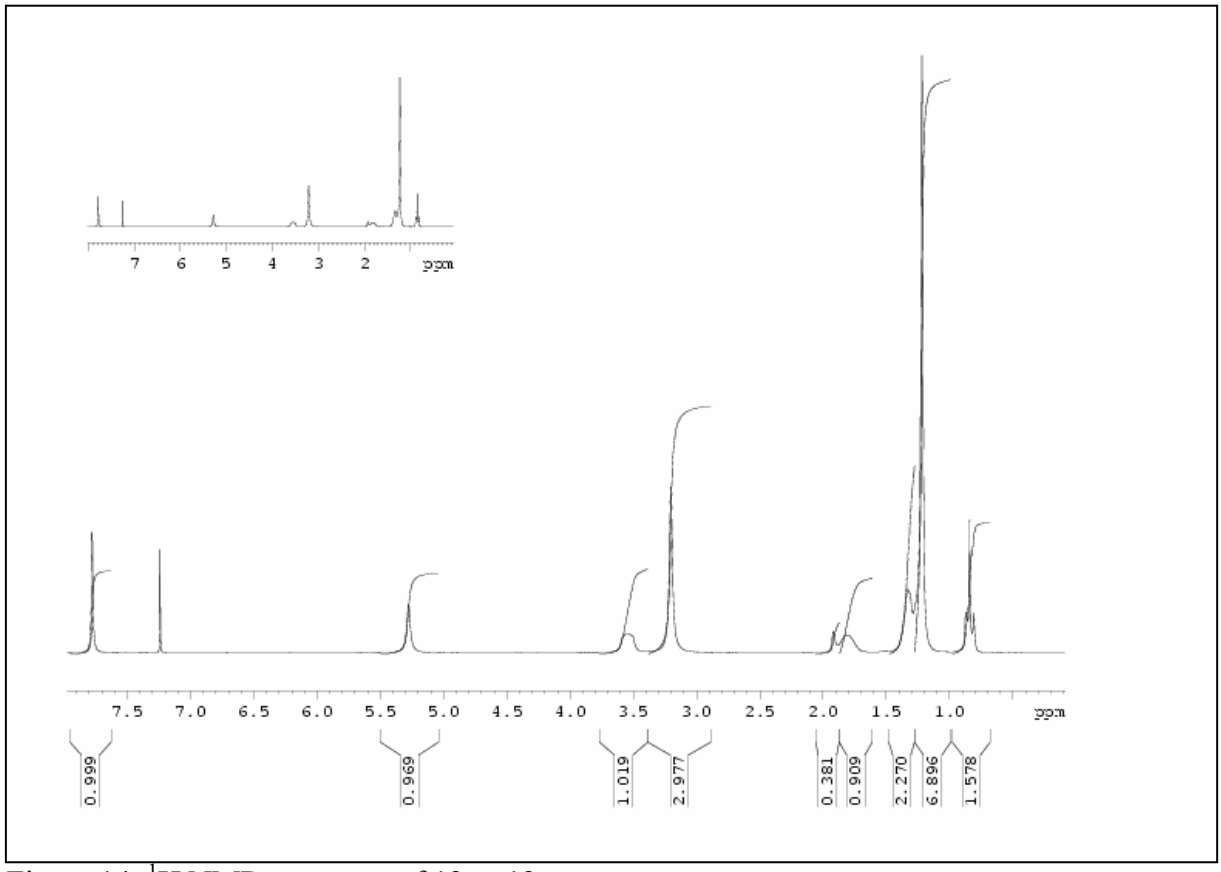

Figure 14: ^{1}H NMR-spectrum of 12-φ-12 .

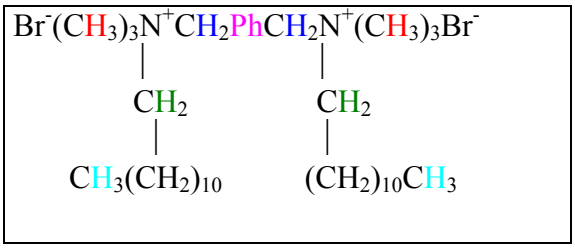

Figure 15: Structure of 12-φ-12.

Protons on phenyl rings, generally are shifted at higher ppm-values (6,5-8,5ppm)[40] than protons on C-atoms bound to N. The peak shifted far to the left is possible due to protons connected to the phenyl ring in the spacer (pink, fig. 15). The second top corresponds to

chloroform (see 6.2.1.1.). The third top is due to protons on C-atoms, which are bound to N and to the phenyl ring (blue, fig. 15).
The fourth top corresponds to protons on C in the tails attached to N (green, fig. 15), the fifth top is due to the methylene-groups on the N-atoms (red, fig. 15). Peak 6 is due to acetone impurities. Peaks 7 and 8 are due to H on C in the tails between the upper C-atom and the bottom CH_3-group (black, fig. 15). The last top corresponds to the CH_3-groups on the ends of the tails (cyan, fig. 15) The integrals are listed in table 6 in appendix.

5.2.2 Mass spectrometry

5.2.2.1 hexanediyl-1,6-bis(dimethyldodecylammonium bromide) (12-6-12)

MS-spectra of 12-6-12 (synthesis 1b)) are shown in figure 16. The intensity (y-axis) of the species are given along the y-axis and characterised with the mass to charge ratio (m/z-value) for the specie along x-axis. The highest peak in the spectrum (base peak), is set to an intensity of 100%, the intensity of the other peaks is relative to the base peak.

Br has two isotopes, ^{79}Br (50,52%) and ^{81}Br (49,48%)[41] and hence Br-containing ions appear with two peaks (at m/z and m/z+2) in the MS spectrum of almost equal intensity. Smaller peaks that follow a larger peak with an increase in mass of an integer are due to isotopes of carbon in the specie.

In the MS-spectrum of 12-6-12 i figure 16, all peaks are single, hence no ions contain Br^-. The base peak in the spectra occurs at m/z=255,3. It corresponds to the diquaternized, divalent ion, which have an expected value of m/z of 255. The following peaks at m/z = 255,8 and 256,4 is due to ^{13}C.

The peak at m/z = 265,3 is due to rests of 12-φ-12, which was running prior to 12-6-12.

If the monoquaternized compound were present, with one bromide attached to it, it would occur as a monovalent ion at m/z=377, but no such peak is seen in the spectrum.

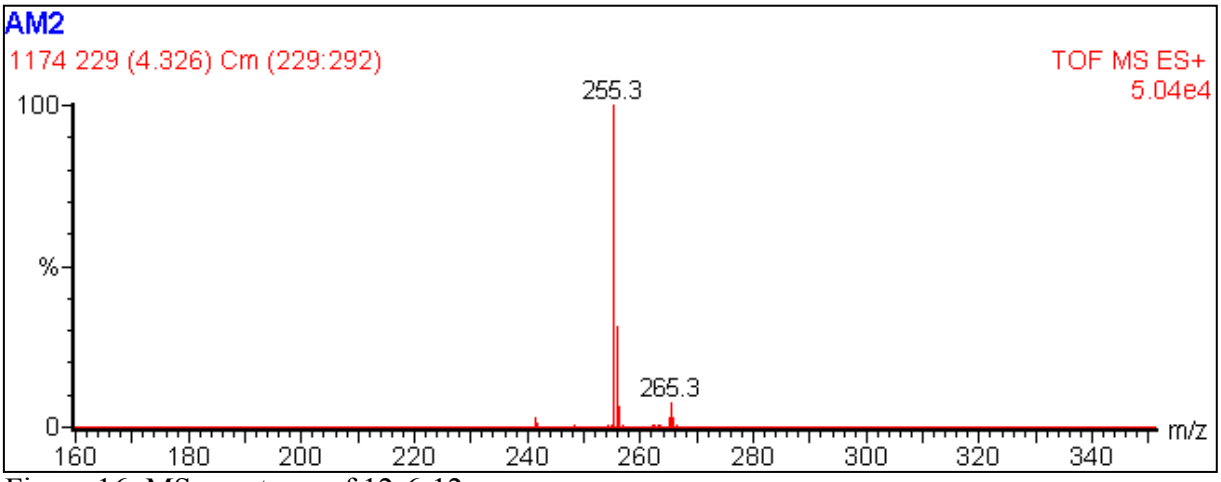

Figure 16: MS-spectrum of 12-6-12.

5.2.2.2. dimethylparaphenyl-α,ω-bis(dimethyldodecylammonium bromide) (12-φ-12)

The MS spectra of 12-φ-12 (synthesis 2b)) are shown in figure 17.

The base peak occur at m/z = 265,3, and correspond to the diquaternized, divalent ion. The calculated m/z is 265. The peak is single, and the ion contains no Br. The following peaks at m/z = 265,8 and 266,3 are due to ^{13}C.

The monoquaternized compound would have occurred with z=1 and m/z = 397, but no such peak is seen.

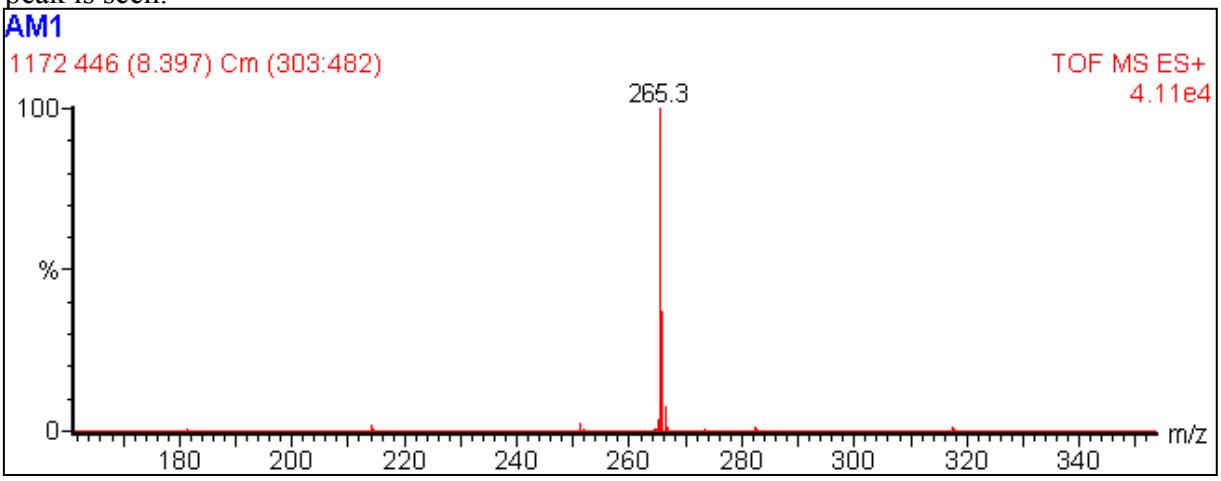

Figure 17: MS-spectrum for 12-φ-12

5.2.3 Melting point determination

The measured melting point of hexanediyl-1,6-bis(dimethyldodecylammonium bromide) (12-6-12) and dimethylparaphenyl-α,ωbis(dimethyldodecylammonium bromide) (12-φ-12) are tabulated in table 4, along vith mean value and standard deviation. The value of T_m obtained for 12-6-12 (T_m = 231±1,$_8$ °C) lie somewhat above the reported melting point of 12-6-12[10] (T_m≈218 °C). This can be due to calibration errors in the thermometer used for the measurements, or due to overheating of the sample near the observed T_m. T_m obtained for 12-6-12 was
T_m = 224±2,$_6$ °C (no reference).

A higher melting point was measured for12-φ-12 than for 12-6-12 (table 4).
12-φ-12 also attains the highest cmc-value of the two (3.1.3.). A similarity between surfactant in the melted state and in the micellar phase is reported for m-s-m surfactants. Both cmc and T_m for m-s-m surfactants attain a maximum at s=5-6, and high T_m and cmc indicates low stability for the surfactant in the melted state and in micelles, respectively[10]. The higher T_m observed for 12-φ-12 perhaps reflects the higher cmc of 12-φ-12 than of 12-6-12.

5.2.4 Solubility of 12-6-12 and 12-φ-12

Solubility in water was compared of hexanediyl-1,6-bis bromide) (12-6-12) and dimethylparaphenyl-α,ω-bis(dimethyldodecylammonium bromide) (12-φ-12) at room temperature. 12-6-12 dissolved spontaneous in water for all prepared solutions (max at ca. 18 mmolal) after some stirring. The Krafft point[10] for 12-6-12 is reported to be 0 °C [], which reflect a high solubility of the surfactant at room temperature. 12-φ-12 did not dissolve in water at 1 mmolal or 8 mmolal, but it dissolved at 0,13 mmolal, after stirring for 1 day. Low

solubility in water at 25 °C for m-φ-m surfactants is reported[22]. The low solubility of 12-φ-12 versus 12-6-12 is perhaps due to low solubility of the phenyl-ring in water (high negative ΔS of solubilisation of benzene in water, 3.1.3.). Poor solubility conditions of 12-φ-12 in water excluded further investigation with the surfactant and polymer (HMHEC).

5.3 Polymer-surfactant interactions

5.3.1 Phase-separation of samples

The phase-separation of 0,2w/w% HMHEC aqueous solutions with 12-6-12 and DoTAB was investigated at room temperature. The solutions were below c* for HMHEC (c*=0,24 g/dl, table 12). The solutions phase-separated i one polymer-rich phase and one polymer depleted phase. The polymer-rich phase was clear, dense and highly viscous, which sedimented in the sample bottles. This phase can be explained by formation of a hydrogel[5]. The upper phase was transparent and low viscous. Similar observations of phase-separation was observed in aqueous systems of HMHPG (hydrophobically modified hydroxypropylguar) with quaternary ammonium surfactants[5]. The phase separation occurring for low surfactant concentration in the semidilute region of HMHEC can be explained by a bridging flocculation of the HMHEC molecules by the added surfactant: The added surfactant aggregate on the hydrophobic groups on the HMHEC molecules which enhance the interchain-bridging of the HMHEC[4,5]. The observed phase-separation in this work occurred for the HMHEC/DoTAB-solutions in the interval 7-17 mmolal DoTAB, and for HMHEC/12-6-12 for 0,3-1,2 mmolal 12-6-12. Hence, both surfactants revealed phase-separation in an interval around CMC.

Samples of HMHEC with DoTAB and 12-6-12, which were semidilute in HMHEC concentration, phase separated after some weeks, after the measurements were carried out. As for the dilute systems (above), the phase-separation occurred for samples with concentrations of surfactant around CMC. The phase-separation seemed to be stronger and appeared after a shorter time for the dilute HMHEC-solutions. Panmai et al.[6] reports on phase separation in semidilute aqueous solutions of HMHEC modified with C_{16} alkyl-chains with added SDS, explained by strong intermolecular interactions that lead to formation of a hydrogel.

5.3.2 Capillary viscosimetry

5.3.2.1 Reduced viscosity[1]

The measurements in capillary viscosimetry (table 7) were carried out on dilute HMHEC-solutions for the systems HMHEC/water, HMHEC/DoTAB/water and HMHEC/12-6-12/water. In the dilute concentration regime of HMHEC, ($c<c^*$), the HMHEC molecules associates intramolecularly through hydrophobic groups along the HEC-sidechain. Intermolecular interactions between the hydrophobic groups[44] can occur at concentrations far below c* (Introduction). In the case of HMHEC, this is rationalised by the rigid HMHEC-backbone[7,46] which leaves HMHEC an extended structure which exposes hydrophobic groups to the aqueous phase, permitting association between hydrohobes on different HMHEC molecules below c*. The interactions in the dilute HMHEC-system are highly dependent on ionic surfactant, by hydrophobic association between the hydrophobic groups on HMHEC and the surfactant tails[3,46].

Reduced viscosity η_{red} was calculated with equation 9 (3.4.2.). The plot of η_{red} against concentration of HMHEC in pure water (fig. 18 a)), show a positive linear trend. A linear trend for η_{red} is also observed for the systems of hm-chitosan with CTAB[47]. A linear trend in the plot of Huggins equation is characteristic for dilute polymer solutions, when the polymer chains have not started to overlap[48]. The increase in η_{red} upon increasing concentration of HMHEC below c*, can be explained by an increase in hydrophobic intermolecular interactions, which is explained in the above text. The plot of η_{red} for HMHEC 2 in pure water (fig. 18 b)) is also increasing linearly in concentration of HMHEC 2, but show a lower slope than for HMHEC. This indicates a lower degree of hydrophobic association in the solutions of HMHEC 2, and a lower degree of hydrophobic modification of HMHEC 2 than HMHEC[49]. S. Nilsson et al. performed measurements in capillary viscosimetry on aqueous solutions of non-ionic cellulose ethers MC (methylcellulose) and the higher hydrophobically modified HPMC (hydroxypropylmethylcellulose), and found a higher slope in η_{red} vs. polymer concentration for the latter. This was explained by stronger interactions between the polymer molecules of the more hydrophobic HPMC than of MC in water[48].

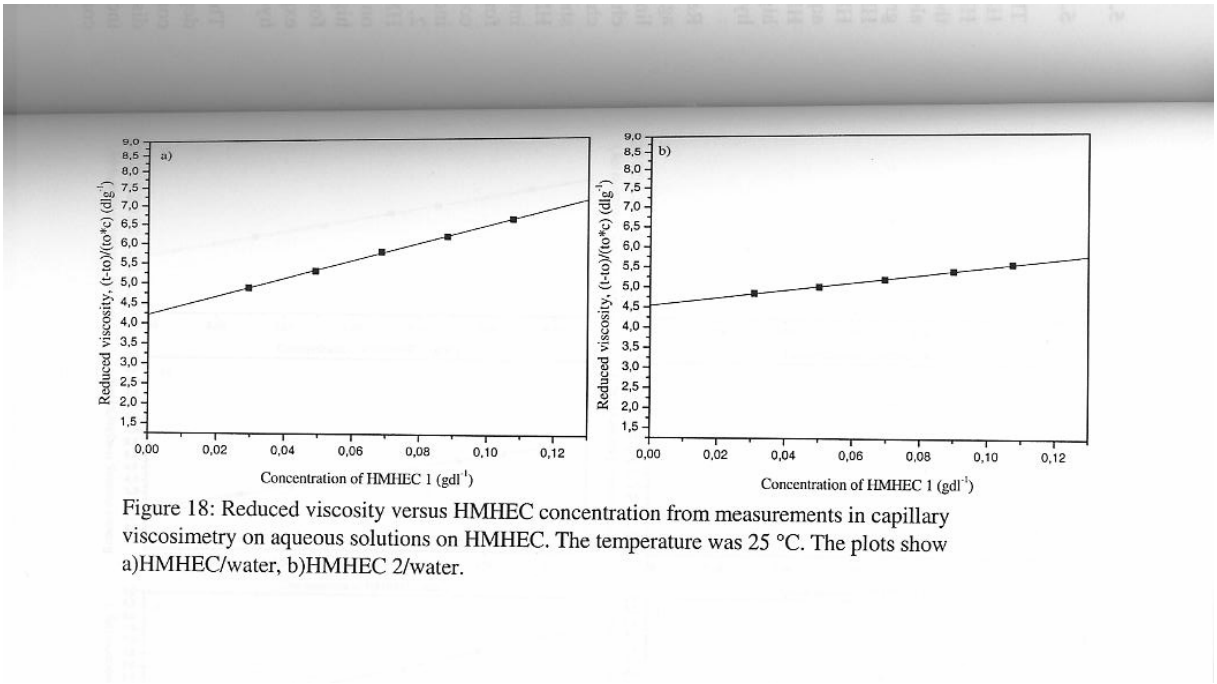

Figure 18: Reduced viscosity versus HMHEC concentration from measurements in capillary viscosimetry on aqueous solutions on HMHEC. The temperature was 25 °C. The plots show a)HMHEC/water, b)HMHEC 2/water.

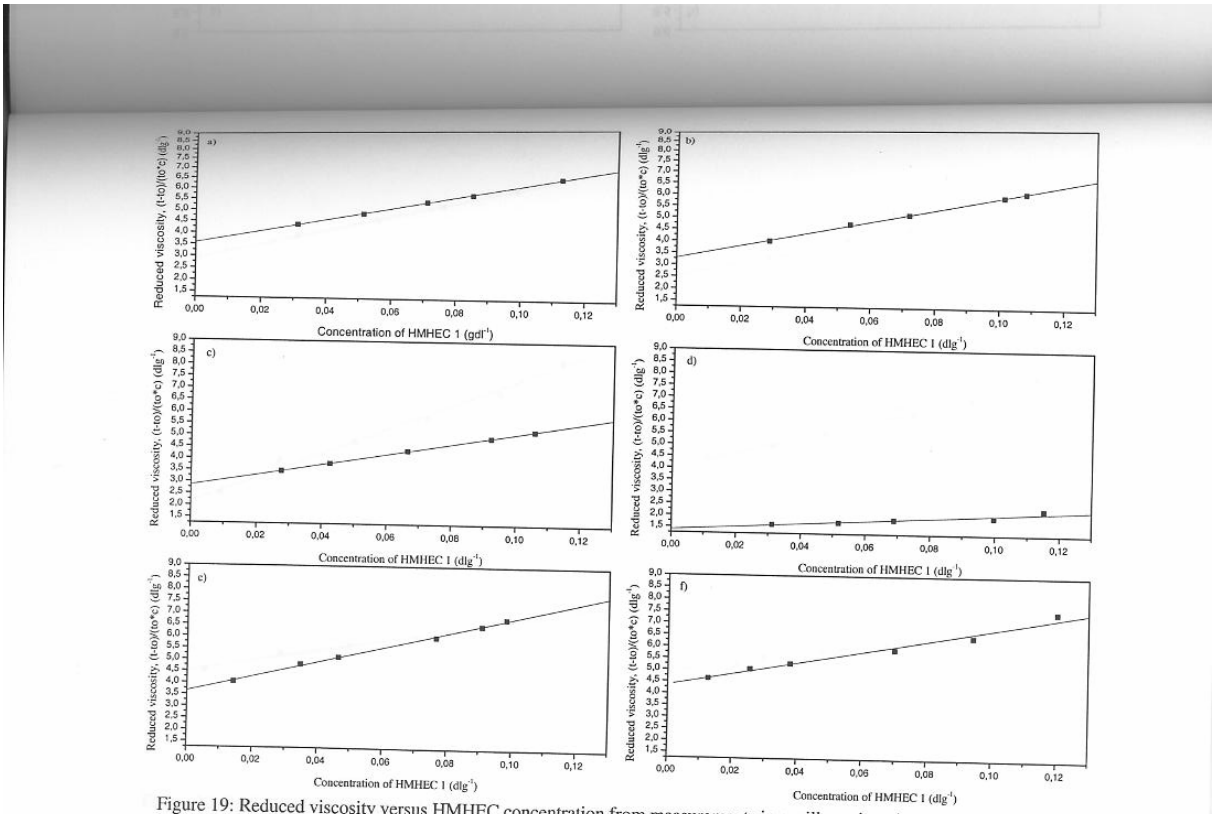

Figure 19: Reduced viscosity versus HMHEC concentration from measurements in capillary viscosimetry on aqueous solutions on HMHEC with DoTAB. The temperature was 25 °C. The plots are for a)1,5 mmolal DoTAB, b)3 mmolal DoTAB, c)6 mmolal DoTAB, d)10 mmolal DoTAB, e)18 mmolal DoTAB, f)20 mmolal DoTAB.

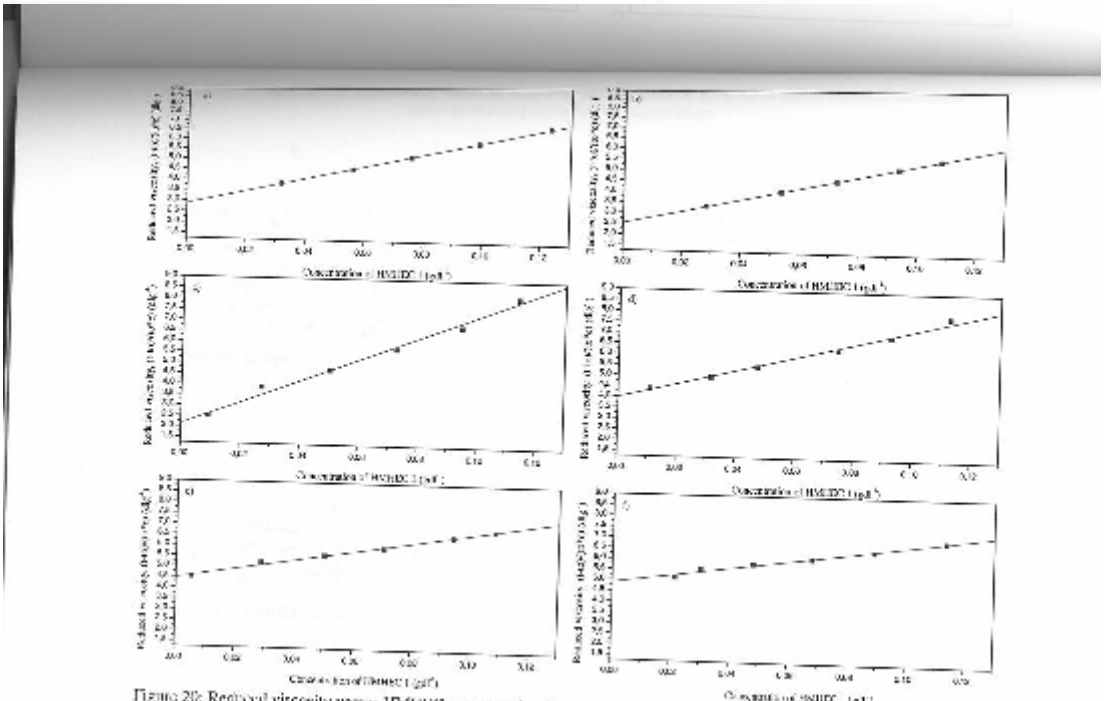

Figure 20: Reduced viscosity versus HMHEC concentration from measurements in capillary viscosimetry on aqueous solutions of HMHEC with 12-6-12. The temperature was 25 °C. The plots are for a)0,15 mmolal 12-6-12, b)0,3 mmolal 12-6-12, c)1,2 mmolal 12-6-12, d)1,5 mmolal 12-6-12, e)3 mmolal 12-6-12, f)6 mmolal 12-6-12

The plots of η_{red} of HMHEC/DoTAB (fig 19) in water, show a linear dependency with a positive slope B (table 11) on increasing the HMHEC concentration. The increase in η_{red} can be pictured as an enhancement in the distribution of surfactant in the solution when the HMHEC concentration increases. In the EHEC-SDS-case[46], an increase in EHEC concentration at a constant SDS concentration leads to an increase in cooperativity between the polymer-chains by an enhanced distribution of SDS on the EHEC in solution. The

increase in cooperativity was followed by and increase in Huggins constant, and hence a larger slope B of Huggins equation (eq. 16). The slope $B = k_H \cdot [\eta]^2$ of η_{red} is plotted vs surfactant concentration in figure 22. For HMHEC/DoTAB, B is increasing going form 0 mmolal to 3 mmolal DoTAB. In the proximity of the region with phase-separation, B show a decrease. This is possibly due to the square-dependency of B on [η] (see above) and the strong decrease in [η]. The solution of HMHEC with 10 mmolal DoTAB, which lies in the region of phase-separation, show a very small slope in η_{red}. The phase-separation led to a reduction in the strength of HMHEC to the solution, which gave the low slope of η_{red} at 10 mmolal DoTAB. The region above of phase separation, B has a larger value than at the onset of the phase-separation. Above the phase-separation, B shows a decrease.

The η_{red} plots for HMHEC with 12-6-12 (fig 20) show the same positive linear trend in concentration of HMHEC, and a region with phase-separation occurring around CMC of 12-6-12. The pattern of the slope B in η_{red} vs 12-6-12 concentration is the same as form DoTAB. B increases from 0 mmolal to 0,15 mmolal 12-6-12, attains a maximum, and show a decrease, which is interrupted by the phase-separation in the region 0,3 – 1,2 mmolal. The region above the phase-separation region starts at a higher value of B than at the beginning of the phase-separation. B then decreases above 1,2 mmolal 12-6-12. The slope B of the solutions in the one-phase-regions is larger than in the case of HMHEC/DoTAB. This implies stronger increase in η_{red} with concentration of HMHEC in the case of 12-6-12, and hence stronger hydrophobic interactions.

The increase in the slope B of η_{red} (fig. 22) in the region before phase-separation occurred could be due to formation of larger aggregates of HMHEC and surfactant in solution induced by increased hydrophobic interaction. In the following phase-separation region, the hydrophobic interactions between HMHEC and ionic surfactant and between the HMHEC-surfactant-aggregates are very strong, which lead to flocculation of the aggregates, which precipitates from the solution. The flocculation can occur by a bridging mechanism through the hydrophobic groups, which is indicated for phase separation upon dilution of aqueous systems of HMEHEC and SDS[4]. The decrease in B after the phase-separation region can be explained by de-aggregation of the HMHEC-surfactant aggregates by surfactant. At a surfactant concentration C_m < CMC, the HMHEC hydrophobic domains are saturated with surfactant[46], and added surfactant lead to disruption of aggregates. The reduction in relative viscosity in dilute aqueous systems of HM-EHEC with SDS is explained by deaggregation of aggregates existing in the solution at low polymer and surfactant concentration[3]. Swelling due to higher Br^- strength and headgroup-repulsion due to the aggregated surfactant lead to

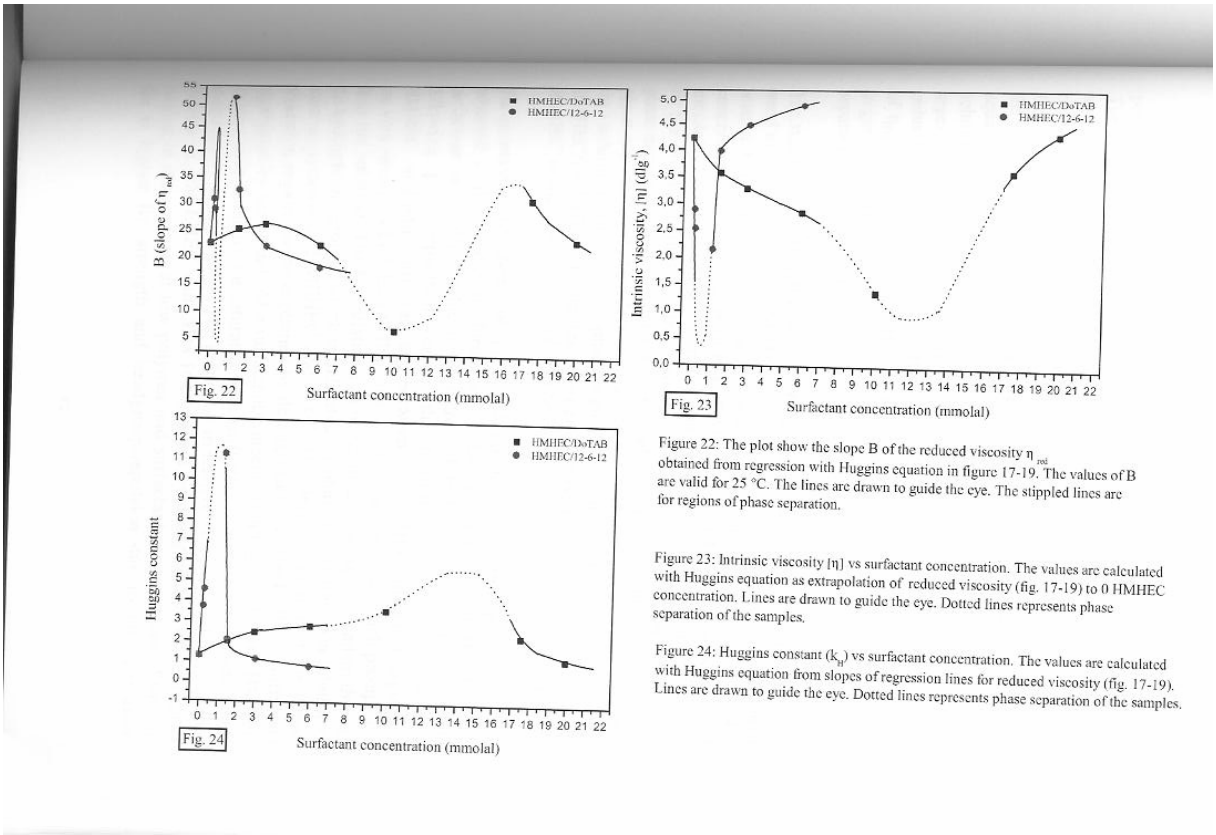

Figure 22: The plot show the slope B of the reduced viscosity η_{red} obtained from regression with Huggins equation in figure 17-19. The values of B are valid for 25 °C. The lines are drawn to guide the eye. The stippled lines are for regions of phase separation.

Figure 23: Intrinsic viscosity [η] vs surfactant concentration. The values are calculated with Huggins equation as extrapolation of reduced viscosity (fig. 17-19) to 0 HMHEC concentration. Lines are drawn to guide the eye. Dotted lines represents phase separation of the samples.

Figure 24: Huggins constant (k_H) vs surfactant concentration. The values are calculated with Huggins equation from slopes of regression lines for reduced viscosity (fig. 17-19). Lines are drawn to guide the eye. Dotted lines represents phase separation of the samples.

extension of the aggregates, and free surfactant micelles (C > CMC)[50] and Br^- can screen hydrophobic interaction between the aggregates, which can further explain the reduction in the slope of η_{red}.

For the η_{red} plots for 1,2 mmolal and 1,5 mmolal 12-6-12 and 20 mmolal DoTAB at the highest HMHEC concentration, η_{red} is higher than expected. It can be ascribed with stronger hydrophobic interactions between aggregates and large aggregates, caused by the high HMHEC-concentration. This is also observed for reduced viscosity for aqueous solutions of HPMC near overlap concentration in water, which was explained by strong interactions between the HPMC-molecules[48]. Higher order terms are needed in Huggins equation at high polymer concentration[48] below c*. The plots of η_{red} of 12-6-12 for 1,2 mmolal, 3 mmolal and 6 mmolal, show a lower reduced viscosity than expected for the lowest HMHEC concentration. This can be due to the high surfactant-HMHEC ratio, and thereby to a deaggregation of aggregates by surfactant. Also the presence of free micelles of 12-6-12 (C >CMC) and Br^- can screen hydrophobic interactions[3,50] and participate in the lowering in η_{red}.

The increase in the strength of hydrophobic association in the dilute systems of HMHEC upon addition of DoTAB and 12-6-12 is predicted by the observed enhanced increase in reduced viscosity. The slope B of η_{red} show largest values for the HMHEC/12-6-12 system, which indicates stronger hydrophobic association between HMHEC and 12-6-12 than for HMHEC with DoTAB.

5.3.2.2 Estimation of intrinsic viscosity [η] and Huggins constant k_H from η_{red}

The reduced viscosity showed linear behaviour of all measured systems of HMHEC with DoTAB and 12-6-12 (5.3.2.). Linear regression on η_{red} , $\eta_{red} = B \cdot c + A$ where A,B are constants and c = concentration of HMHEC in g/dl was fitted to Huggins equation (eq. 16),

and from this, [η] and k_H were estimated. The values of [η] are the values of the intercept A, extrapolated values of η_{red} to zero HMHEC-concentration. The values of k_H were obtained from the intercept A and the slope B through $k_H = B/A^2$.

5.3.2.3 Discussion of [η] and k_H

Intrinsic viscosity [η] (eq. 11-13, 3.4.2.) measures specific volumes of polymer molecules in solutions approaching zero polymer concentration. The plot of intrinsic viscosity [η] (fig 23) against surfactant concentration show a decrease in [η], interrupted by a region of phase separation in an interval around CMC, followed by an increase in [η] for both HMHEC/DoTAB and HMHEC/12-6-12. The decrease in [η] is attributed to a contraction of polymer chains, which is concluded by others in aqueous systems of hm-polymer with and without added ionic surfactant[49,46,47]. From equation 12 (3.4.2.), the hydrodynamic volume V_h is expected to decrease in decreasing [η]. The reduction in [η] appear simultaneously with a rise in Huggins constant k_H (fig. 24) upon the increase in surfactant concentration. k_H measures of the strength of polymer-polymer and polymer-solvent interactions in aqueous polymer systems, and high values of k_H implies strong coil-coil interactions and a poor solvent quality[47]. k_H obtains values between 0,3 and 0,8 for random coil polymers[42]. The values of k_H in table 12 lies above 0,8, unless for HMHEC 2/water and HMHEC/6mmolal 12-6-12. This indicates very strong hydrodynamic interactions in the solutions. High values of k_H are also reported in other aqueous systems of hm-polymer[49] and for aqueous systems of hm-polymer with ionic surfactant[46,47]. The simultaneous decrease in [η] and increase in k_H is observed for hm-chitosan with CTAB[47]. This was explained by an increase in hydrophobic intramolecular interactions, due to larger enhancement in k_H for the more hydrophobically modified chitosan-polymer upon CTAB-addition. For aqueous systems of copolymer of AM and AAM, [η] decreased and k_H increased upon increasing amount of AAM in the polymer[49]. It was explained by an increase in intramolecular interaction, leading to contraction of the coils, and possibly intermolecular interactions, according to the increase in k_H. For the systems under investigation in this work, the region of decrease in [η] and increase in k_H ends with phase-separation, which indicates strong interactions between the HMHEC-surfactant complexes. For EHEC with SDS[46], the parallel increase in k_H and decrease in [η] is explained by the expanded structure of EHEC, which lead to interassociation between the hydrophobic groups on EHEC and SDS, which lead to a more compact conformation of EHEC. The increase in k_H was explained by higher hydrodynamic interactions upon increased EHEC concentration due to stronger polymer-polymer interactions by an increase in the average aggregation number. The phase-separation observed for HMHEC with surfactant can then be rationalised by an increase in hydrophobic intermolecular interactions for the extended HMHEC chains on addition of DoTAB or 12-6-12 that compacts the HMHEC-coils more and more until it escapes from the aqueous phase. The increased Br^- concentration from the dissociation of DoTAB and 12-6-12 in the solution lead to poorer conditions for HMHEC, which can participate in the contraction of the HMHEC-coils.

The end of the phase-separation region can be understood as a de-aggregation of the large phase-separated HMHEC-surfactant aggregates by enhanced electrostatic repulsion between the surfactant headgroups as the surfactant concentration increases. Deaggregation of EHEC-SDS-aggregates in dilute EHEC aqueous solution at elevated SDS-concentration is observed by light scattering by S. Nilsson et al.[3]. Above the region of phase-separation, the [η] increases (fig. 23) and k_H decreases (fig. 24), which indicates larger HMHEC-surfactant-complexes along with decreasing hydrodynamic interactions and better solvent-quality. The

increase in size of the HMHEC-surfactant complexes can be explained by extension of the aggregates due to electrostatic repulsions as the surfactant concentration is further increased. The enhanced Br- strength lead to swelling and further extension of the aggregates. The decrease in k_H in the same region is rationalised by screening of hydrophobic interactions between the HMHEC-surfactant-aggregates by repulsion between the polyelectrolyte-like HMHEC-surfactant-aggregates. The reduction in k_H also reflects the better solvent- conditions for the polyelectrolyte-like aggregates of HMHEC with DoTAB or 12-6-12.

[η] is showing a levelling off at the highest surfactant concentrations. This can be due to free micelles of DoTAB and 12-6-12 (C > CMC), that can screen the electrostatic repulsion[3] between the HMHEC-surfactant aggregates, and thereby lead to a weakening in the [η]-increase. The ionisation-degree of free micelles is reported to be lower than in the case of polymer-bound micelles in the case of diblock copolymer of PEO-PPO with SDS[20]. In the case of HMHEC with DoTAB and 12-6-12 a lowering in ionisation degree of the free micelles above CMC contra the polymer-bound micelles can give a lowering in the swelling effect, and hence contribute less to the extension of the aggregates. An illustration of the effect of addition of ionic surfactant to dilute aqueous solution of hm-polymer is shown in figure 21.

Figure 21: Illustration of association between HMHEC and DoTAB or 12-6-12 in dilute aqueous solutions upon increasing surfactant concentration.

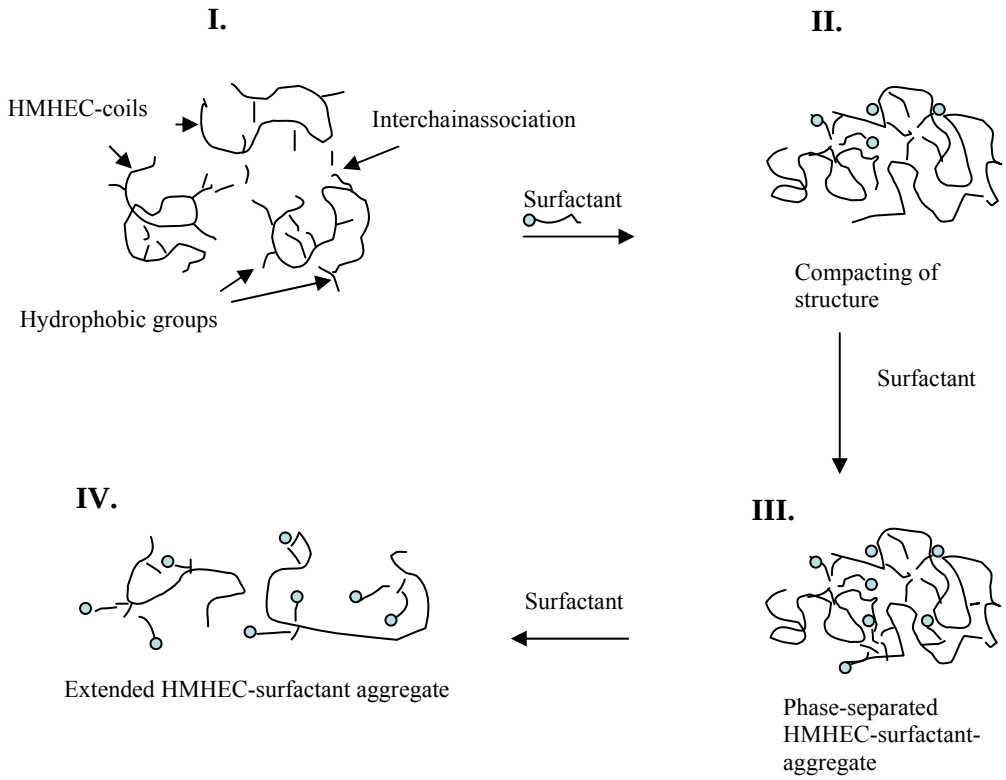

5.3.2.4 Comparing of [η] and k_H for DoTAB and 12-6-12.

The effect of surfactant-addition on [η] and k_H for the dilute HMHEC solutions is most pronounced with 12-6-12. k_H attains higher values and [η] attains lower values for HMHEC/12-6-12 than for HMHEC/DoTAB, which implies stronger hydrodynamic

interactions in the system of HMHEC/12-6-12. The curves are situated at lower surfactant concentrations for 12-6-12 than for DoTAB. For aqueous systems of hyaluronic acid with 12-s-12-surfactant and DoTAB, the interactions occurred at lower surfactant concentration with 12-s-12 than with DoTAB[15]. This is attributed to the lower CMC of 12-6-12 (≈ 1 mmolal) than of DoTAB (≈ 16 mmolal) (3.1.1.). The change in [η] and k_H in surfactant concentration is much larger for HMHEC/12-6-12, which reflects a more co-operative aggregation of 12-6-12 to HMHEC than of DoTAB to HMHEC. Microcalorimetric studies[13] of interactions in aqueous solutions of N,n-alylacrylamide with 12-6-12 and DoTAB revealed that the formation of mixed micelles was entropy-driven, and that ΔS of the process was larger of 12-6-12 than of DoTAB with the polymer. Stronger interaction between 12-s-12-surfactants than of DoTAB with hyaluronic acid in water is reported[15]. Isothermal calorimetric measurements on hydrophobically modified HASE-polymer and SDS showed that the entropy of the interaction between polymer and SDS increased with increasing hm-degree of the polymer[14]. Stronger interaction of HMHEC with 12-6-12 than with DoTAB can then be rationalised by the higher hydrophobicity of 12-6-12 due to the hydrophobic spacer-chain (3.1.1.). The rapid decrease in[η] before phase-separation occur implies a stronger compatibility of 12-6-12 to contract the HMHEC-surfactant aggregates. It can be thought of as a result of that each molecule consist of two hydrophobic alkylchains rather than one as for DoTAB, and hence that each molecule of 12-6-12 is more effective in the contraction of the HMHEC-coils, in combination with stronger hydrophobic interaction, as mentioned above. The lower Br^- concentration for HMHEC/12-6-12 than of HMHEC/DoTAB may also less have disturbed the very strong contraction of the HMHEC-aggregates. The corresponding strong increase in [η] above the phase-separation of HMHEC/12-6-12 implies a strong repulsive effect of 12-6-12, which can be attributed to the large size of the headgroup of 12-6-12 compared with DoTAB. The levelling off in [η] is more marked for HMHEC/12-6-12 than of HMHEC/DoTAB. It can be explained by the general larger changes in intrinsic viscosity in surfactant concentration, as a result of the larger cooperativity of the HMHEC/12-6-12-system

5.3.3 Shear viscosimetry

5.3.3.1 Estimation of zero-shear viscosity η_0 and critical shear-rate $(d\gamma/dt)_c$ from flow-curves of η

Zero shear viscosity η_0 for aqueous solutions of HMHEC/DoTAB and HMHEC/12-6-12 (table 15) is estimated from the flow curves, showing apparent viscosity η vs shear rate dγ/dt. η_0 was the mean value of the measured values of η in the Newtonian plateau. The measuring points in the plateau were chosen as the values of η which deviated less than 5% from the η measured at lowest dγ/dt.

The values of $(d\gamma/dt)_c$ were regarded as the values of dγ/dt at the onset of shear thinning in the plots of η (figs. 25, 26), and were taken as the last value of η in the Newtonian plateau defined above for estimation of η_0.

5.3.3.2 Discussion of critical shear rate $(d\gamma/dt)_c$ and zero-shear viscosity η_0

The rheological measurements were carried out on HMHEC solutions in the semidilute regime, where c (HMHEC) > c* (overlap concentration). c* of HMHEC in water was estimated to c* ≈ 0,24 g/dl. (table 12), and the samples had a HMHEC concentration of ≈ 0,72

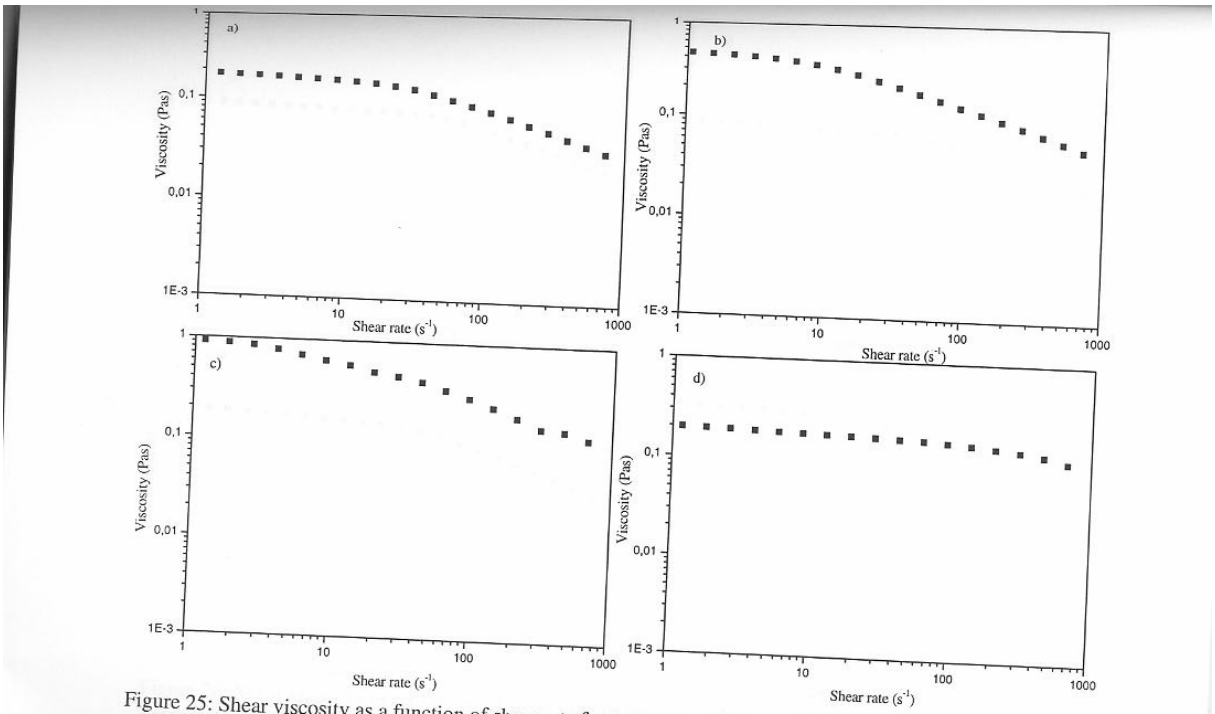

Figure 25: Shear viscosity as a function of shear rate for aqueous solutions of 0,72gdl^{-1} HMHEC with DoTAB. Temperature 25 °C. The plots show a)5 mmolal, b)10 mmolal, c)15 mmolal, d)20 mmolal DoTAB.

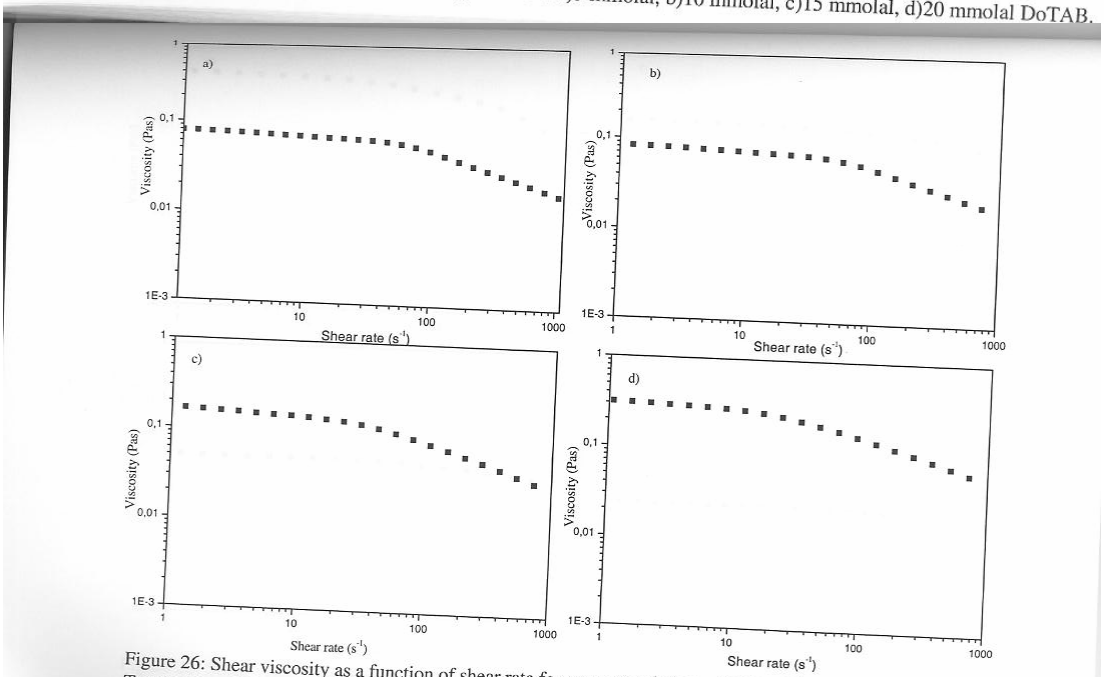

Figure 26: Shear viscosity as a function of shear rate for aqueous solutions of 0,72gdl^{-1} HMHEC with 12-6-12. Temperature 25 °C. The plots show a) 0 mmolal, b)0,15 mmolal, c)0,6 mmolal, d)0,75 mmolal 12-6-12.

g/dl. In the samples, the HMHEC-coils were possibly overlapping, forming a transient network through entanglements and by association between the hydrophobic sidechains in tie-points[1,2,3,7]. By introduction of ionic surfactant (DoTAB and 12-6-12), also Coulomb repulsion due to the charged surfactant headgroups, and hydrophobic interaction between the hydrophobic groups on HMHEC and the tails on the surfactant contributed come into play.

The plots of shear viscosity η versus shear rate dγ/dt (fig. 25, 26) show shear thinning behaviour for all solutions of HMHEC/water, HMHEC/ DoTAB and HMHEC/12-6-12. Shear thinning is also observed by others in shear experiments on aqueous solutions of HMHEC [2],

and in aqueous systems of hyaluronate with DoTAB[15], where shear thinning was ascribed with disruption of network in solution. Shear thinning is a typical phenomenon in systems with transient networks[44]. The shear thinning observed for HMHEC/water is probably due to disruption of hydrophobic associations between the hydrophobic side chains on HMHEC and of entanglements. The critical shear rate $(d\gamma/dt)_c$, which marks the onset of the shear thinning, is reported to decrease in increasing surfactant concentration for C < CMC (fig. 27) for both HMHEC/12-6-12 and HMHEC/DoTAB. This lowering in $(d\gamma/dt)_c$ leads to an increase in the inverse value (eq. 24, 3.5) the longest relaxation time τ^* of the system, which is correlated to the relaxation of the whole network. The observed decrease in $(d\gamma/dt)_c$ is attributed to shorter length between the tie points in the network along with the increase in surfactant addition. The added surfactant aggregate on the hydrophobic domains on HMHEC to form mixed micelles at surfactant concentrations above CAC (Introduction). The addition of surfactant lead to, first a strengthening of each network point in the network formed in absence of surfactant, by increased hydrophobic interaction. Second, it give an increase in the number of network points by an increased bridging of the hydrophobic groups on HMHEC by surfactant to a more tight network with smaller mesh-size. The decrease in $(d\gamma/dt)_c$ is followed by an increase in zero shear viscosity η_0 (fig. 28) at surfactant concentrations below CMC. A maximum in zero shear viscosity somewhat below CMC, which is observed in other systems of hydrophobically modified polymer with cationic surfactant[3,7,51]. The increase in η_0 can be understood by the formation of a more connected transient network. At concentration of surfactant above CMC, the solutions show almost no shear thinning, which is coincident with a saturation of the polymer with surfactant, which is to occur when the total amphihpile concentration equals CMC[46]. The lowering in the shear thinning is followed by a decrease in η_0. This is rationalised by a masking of the hydrophobic groups on HMHEC by surfactant micelles, by a solubilisation of each hydrophobe on HMHEC in its own surfactant micelles. This destroy the connectivity in the solution and disrupts the network. Formation of free micelles above CMC and the increasing Br^- concentration can also act to screen interactions between the HMHEC-chains and hence participate in the decrease in η_0.The effect of addition of ionic surfactant to semidilute aqueous solutions of hm-polymer is illustrated in figure 29.

5.3.3.3 Comparing of $(d\gamma/dt)_c$ and η_0 for DoTAB and 12-6-12

The values of critical shear rate $(d\gamma/dt)_c$ (fig. 27) below CMC are lower for HMHEC/12-6-12 than for HMHEC/DoTAB, which indicates higher values of the inverse value τ^* of the former system. A higher τ^* implies a more open network-structure with longer polymer strand-lengths, which needs longer time to relax the applied strain in the case of HMHEC/12-6-12. A more open network structure implies a lower number of network points for HMHEC/12-6-12 than for HMHEC/DoTAB at the interaction maximum around CMC. The maximum value of zero-shear viscosity η_0 is lower for HMHEC/12-6-12 than of HMHEC/DoTAB, which indicates a lower connectivity in the former system. The lower connectivity of HMHEC/12-6-12 can be understood by the actual lower concentration of 12-6-12 than of DoTAB in the system. A more open network structure for HMHEC/12-6-12 can also be due to disruption of the network by sterical hindrance due to the larger headgroup of 12-6-12 than of DoTAB. The decrease in η_0 (fig. 28) with surfactant addition above the maximum is larger for HMHEC/12-6-12, and the reduction in shear thinning behaviour is largest for this system (fig. 26). This indicates a stronger tendency of 12-6-12 to disrupt the network structure, which could be due to the large head group of 12-6-12. The size of the micelles in aqueous solution are reported to be larger for 12-6-12 than for DoTAB (3.1.1.), and if this is also true in the

presence of HMHEC, it can participate in formation of a more open structure to the network

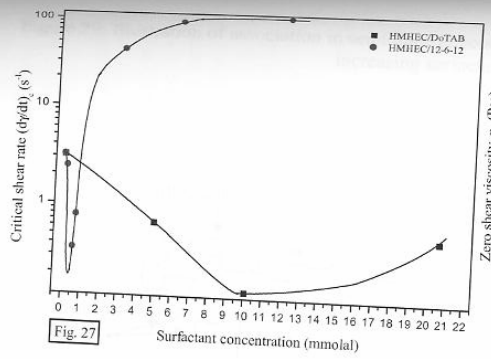

Fig. 27

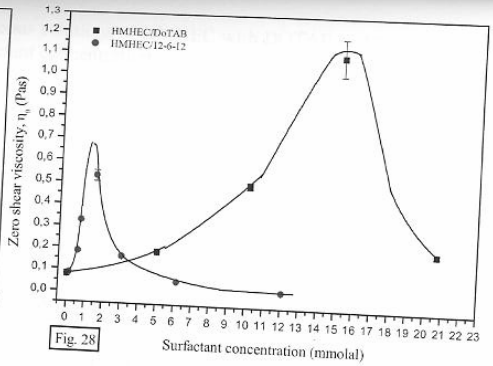

Fig. 28

Figure 27: Critical shear rate $(d\gamma/dt)_c$ versus surfactant concentration for aqueous solutions of 0,72 gdl^{-1} HMHEC with DoTAB or 12-6-12. The lines are drawn to guide the eye. The values of $(d\gamma/dt)_c$ are the values of the shear rate (table 13) at the onset of shear thinning taken from the plots of apparent (shear) viscsity vs. shear rate for aqueous systems of HMHEC with DoTAB and 12-6-12. The data are valid for 25 °C.

Figure 28: Zero-shear viscosity η_0 versus surfactant concentration for aqueous solutions of 0,72gdl^{-1} HMHEC with DoTAB or 12-6-12. The lines are drawn to guide the eye. The η_0 values are the mean value (table 15) of the shear viscosity against shear rate in the Newtonian plateau (figure 19 and 20). The error in the measuring points are 97,5% confidence intervals, calculated based on the standard deviation.

Figure 29: Illustration of association in semidilute aqueous solutions of HMHEC with DOTAB or 12-6-12 upon increasing surfactant concentration.

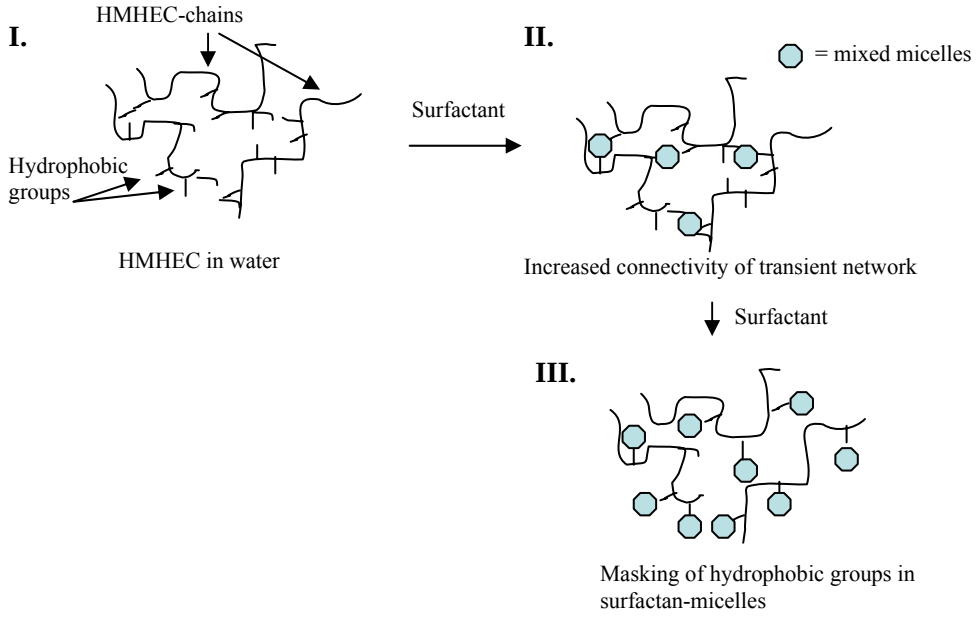

of HMHEC/12-6-12. In the case of 12-6-12 in aqueous solutions of PPO-PEO-copolymer, the size of the mixed micelles were almost constant in polymer concentration, and had only a little lower aggregation number than in pure water (3.1.1.). It is possible to assume that the rigid HMHEC-molecules lead to formation of mixed micelles of lower aggregation number than in pure water.

The changes in η_0 with surfactant concentration is larger for HMHEC/12-6-12 than of HMHEC/DoTAB. This implies larger co-operativity in the HMHEC/12-6-12 system, which indicates stronger adsorption of 12-6-12 to HMHEC than in the case of DoTAB, and again stronger hydrophobic interactions between the hydrophobic groups on HMHEC and the 12-6-12 molecules in the mixed micelles than in the case of HMHEC/DoTAB. Stronger hydrophobic interactions between HMHEC and 12-6-12 than between HMHEC and DoTAB was also concluded from the measurements in capillary viscosimetry (5.3.2.4.). The region of interaction between HMHEC and 12-6-12 is situated at far lower surfactant concentrations than in the case of HMHEC/DoTAB, which can be seen from η_0 (fig. 28), [η] (fig. 23) and k_H (fig. 24). This is correlated to the lower CMC of 12-6-12, which lead to onset of aggregation with HMHEC at lower concentration in 12-6-12 than in DoTAB.

6 CONCLUSION

6.1 Hydrophobic modification on HEC

HEC was hydophobically modified from HEC and bromotetradecane in a homogeneous reaction with NaOH as activating agent. The degree of hydrophobic modification of the

synthesised HMHEC 2 was compared with a commercial HMHEC by capillary viscosimetry. A plot of reduced viscosity versus HMHEC concentration for HMHEC and HMHEC 2 in water show a larger increase in reduced viscosity with HMHEC concentration for the former. This is explained by a higher degree of hydrophobic modification of HMHEC than of the synthesised HMHEC 2.

6.2 hexanediyl-1,6-bis(dimethyldodecylammonium bromide) (12-6-12) and dimethylparaphenyl-α,ω-bis(dimethyldodecylammonium bromide) (12-φ-12)

Two bis (quaternary ammonium bromide surfactants), hexanediyl-1,6-bis(dimethyldodecylammonium bromide) (12-6-12) and dimethylparaphenyl-α,ω-bis(dimethyldodecylammonium bromide) (12-φ-12),were synthesised, and compared by melting point and solubility in water. 12-6-12 had a much higher solubility in water at room temperature than 12-φ-12 (5.2.4.). Interactions of aqueous solutions of HMHEC with 12-φ-12 was not investigated due to the poor water solubility of 12-φ-12. The melting point of 12-φ-12 was found to be higher than of 12-6-12, and this is related to the higher CMC of 12-φ-12 than of 12-6-12 (5.2.3.), according to similarities of the micelle aggregates and the melted state.

6.3 Capillary viscosimetry

The plots of reduced viscosity η_{red} in dilute aqueous solutions of HMHEC with dodecyltrimethylammonium bromide (DoTAB) and HMHEC with hexanediyl-1,6-bis(dimethyldodecylammonium bromide) (12-6-12) showed linear dependency in concentration of HMHEC, in accordance with Huggins equation (eq. 15). η_{red} showed stronger dependency of HMHEC-concentration for HMHEC/12-6-12 than HMHEC/DoTAB. Intrinsic viscosity [η] and Huggins constant k_H were obtained from regression on η_{red} with Huggins equation. [η] showed a decrease and k_H showed an increase vs surfactant concentration below CMC. This region was followed by a region with phase-separation centred in a surfactant concentration interval about CMC. Above the phase-separation region [η] increased and k_H decreased in surfactant concentration.

The plots of [η] and k_H appeared at lower surfactant concentration for HMHEC/12-6-12 than of HMHEC/DoTAB, attributed to the lower CMC of 12-6-12. [η] attained lower values and k_H attained higher values for HMHEC/12-6-12 than of HMHEC/DoTAB. The changes in [η] and k_H in surfactant concentration were much stronger and occurred in a narrower concentration interval for HMHEC/12-6-12 than of HMHEC/DoTAB. The differences for the two systems can be due to stronger hydrodynamic interactions in the system of HMHEC/12-6-12 than of HMHEC/DoTAB and more co-operative association between 12-6-12 and HMHEC.

6.4 Shear viscosimetry

Shear viscosity measurements were performed on aqueous semidilute solutions of HMHEC in water and with dodecyltrimethylammonium bromide (DoTAB) and HMHEC with hexanediyl-1,6-bis(dimethyldodecylammonium bromide) (12-6-12). The flow curves showed

shear thinning for all systems investigated. The critical shear rate $(d\gamma/dt)_c$, which mark the onset of the shear thinning region, decreased in increasing surfactant concentration below CMC. The decrease in $(d\gamma/dt)_c$ lead to an increase in the longest relaxation time, τ^*, of the system. This occurred simultaneous with an increase in zero-shear viscosity η_0. It was ascribed with an increase in the number of network point of the system by aggregation of surfactant on the hydrophobic domains on HMHEC. Above CMC, the systems showed almost no shear thinning, and η_0 decreased. This was attributed to a masking of the hydrophobic groups on HMHEC in surfactant micelles.

The maximum-value of η_0 was highest, and the values of $(d\gamma/dt)_c$ were higher for HMHEC/DoTAB than of HMHEC/12-6-12. This was explained by less connectivity in the system of HMHEC/12-6-12, which can be due to the lower surfactant concentration of 12-6-12 and to the larger headgroup and the larger micelles formed by 12-6-12, which can disrupt the transient network in solution. The curve for η_0 occurred over a narrower concentration interval and was situated at lower surfactant concentration for HMHEC/12-6-12 than for HMHEC/DoTAB. These trends were also observed for $[\eta]$ and k_H (6.3).

7 REFERENCES

1.“The structure and rheology of Complex Fluids”/R. G. Larson, Oxford University Press, New York, USA, 1999

2. “Synthesis and Solution Properties of Hydrophobically Modified (Hydroxyethyl) cellulose”/Sau and Landoll/Polymers in Aqueous Media, American Chemical Society, 1989

3. “Association Phenomena in Aqueous Solutions of Surfactants and Hydrophobically Modified Polymers”/Susanne Nilsson, 1999

4. “Phase separation by dilution in a system of a hydrophobically modified polymer”/K. Thuresson, F. Joabsson/Colloids and Surfaces A, 1999, 151, 513

5. “Interactions between Quaternary Ammonium Surfactant Oligomers and Water-Soluble Modified Guars”/Journal of Colloid and Interface Science, 1999,218, 468

6.”Rheology of hydrophobically modified polymers with spherical and rod-like surfactant micelles”/ Santipharp Panmai, Robert K. Prud′homme, Dennis G. Peiffer, Colloids and Surfaces
A, 147,1999, p.3-15

7. “Interactions between Hydrophobically Modified Polymers and Surfactants: A Fluorescence Study”/S. Panmai, R. K. Prud′ homme , D. G. Pfeiffer, S. Jockusch, N. J. Turro/Langmuir, 2002, 18, 3860

8. “Interaction of Hydrophobically Modified (Hydroxyethyl)cellulose with Various Added Surfactants”/R. Tanaka, J. Meadows, P.A.Williams, G.O.Phillips/Macromolecules, 1992, 25, 1304

9. “Mixed solutions of Surfactant and Hydrophobically Modified Polymer. Controlling Viscosity with Micellar Size.”7S. Nilsson, K. Thuresson, P. Hansson, B. Lindmann/J. Phys. Chem, 1998, 102, 7099

10. “Dimeric (Gemini) Surfactants: Effect of the Spacer Group on the Association Behaviour in Aqueous Solution/R. Zana/Journal of Colloid and Interface Science, 2002, 248, 203

11. “Alkanediyl-α,ω-bis(dimethylalkylammonium bromide) Surfactants.9. Effect of the Spacer Carbon Number and Temperature on the Enthalpy of Micellization”/L. Grosmaire et al. /Journal of Colloid and Interface Science, 2002, 246,175

12. “Dimeric and oligomeric surfactants. Behaviour at interfaces and in aqueous solution: a review”/Raoul Zana/ Advances in Colloid and Interface Science, 2002, 97, 205

13.”Thermodynamics of Interaction between Cationic Gemini Surfactants and Hydrophobically Modified Polymers in Aqueous Solutions”/G. Bai, Y. Wang, H. Yan, R.K. Thomas, J. C.T. Kwak, J.Phys. Chem.B, 2002,106,2153

14. “Model Alkali-Soluble Associative (HASE) Polymers and Ionic Surfactant Interactions Examined by Isothermal Titration Calorimetry”/Seng et al./Langmuir, 2000, 16, 2151

15. “Viscometric study of the sodium hyaluronate-sodium chloride-alkyl-(n)-ammonium surfactant system”/M. Pisarcik et al./Colloids and Surfaces, 1999, 150,207

16. “Aberrant Aggregation Behaviour in Cationic Gemini Surfactants Investigated by Surface Tension, Interfacial Tension and Fluorescence Methods”/Rosen et al/Langmuir, 1999, 15, 7340

17. “Aggregation number of alkanediyl-α,ω-bis(dimethylalkylammonium bromide) surfactants determined by static light scattering”/M. Pisarcik et al./Colloids and Surfaces A, 2000, 172, 139

18. “Microcalorimetric studies on the Thermodynamic Properties of Cationic Gemini Surfactants”/Bai et al./ Langmuir,2001, 17, 4501

19. “Dynamic light scattering and electrokinetic potential of bis(quaternary ammonium bromide) surfactant micelles as the function of alkyl chain length”/Colloids and Surfaces A, 1998, 143, 69

20. “Studies of the Interaction of Cationic Gemini Surfactants with Polymers and Triblock Copolymers in Aqueous Solution”/Journal of Colloid and Interface Science, 2001,244, 377

21.”Gemini Surfactants: A New Class of Self-Assembling Molecules”, ”, F.M. Menger and C.A. Littau , Journal of American Chemical Society, 1993, 115,10083

22. “Surface Properties, Micellization, and Premicellar aggregation of Gemini Surfactants with Rigid and Flexible Spacers”/Song and Rosen/Langmuir, 1996,12,1149

23. “Principles of Colloid and Surface Chemistry”/Hiemenz and Rajagopalan/
3. Ed.

24. “Elongated Aggregates Formed by Cationic Gemini Surfactants”/Oda et al./Langmuir, 1999, 15, 2384

25. “Gemini Surfactants”/ F.M. Menger and C.A. Littau/Angewandte Chemie, 2000, 39, 1906

26. “Alkanediyl-α,ω-bis(dimethylalkylammonium bromide) Surfactants. 3. Behaviour at the Air-Water Interface”/E. Alami, G. Beinert, P. Marie, R. Zana/Langmuir, 1993, 9, 1465

27. “ Alkanediyl-α,ω-bis(dimethylalkylammonium bromide) Surfactants. 1. Effect of the spacer chain length on the critical micelle concentration and micelle ionization degree”/Zana et al. /Langmuir, 1991, 7, 1072

28. “Comparative Rheological Behaviour of Some Cellulosic Ether Derivatives”/El Ghzaoui et al. /Langmuir, 2001, 17, 1453,

29. “Alkanediyl-α,ω-bis(dimethylalkylammonium bromide) Surfactants. 5. Aggregation and Microstructure in Aqueous Solutions.”/Langmuir, 1995, 11,

30. “Fluorescence Probe Study of the Effect of Concentration on the State of Aggregation of Dodecylalkyldimethylammonium Bromides and Dialkyldimethylammonium Chlorides in Aqueous Solution”/R. Zana/Journal of Colloid and Interface Science, 1983, 91 (1), 276

31. “Fluorescence Study of Premicellar Aggregation in cationic Gemini Surfactants/Mathias et al./Langmuir, 2001, 17, 6147

32. “Unusual Structure in Layers of Cationic Gemini Surfactants Adsorbed at the Air/Water Interface: A Neutron Reflectivity Study”/Li et al. /Langmuir, 2002, 18, 6614

33. “Geminisurfactants with Acetylenic Spacers”/Menger et. Al/Langmuir, 2000, 16, 2062

34. ”Dimeric (gemini) Surfactants”/Raoul Zana, “Novel Surfactants”:
Preparation and Biodegradability, Surfactant Science, Vol. 74, Krister Holmberg, Ed. 1998

35. “Neutron reflectivity Studies of the Surface Excess of Gemini Surfactants at the Air-Water Interface”/Li et al./Langmuir, 1999, 15, 4392

36. “Thermodynamic Studies of Aqueous m-s-m Gemini Surfactant Systems”/Journal of Colloid and Interface Science, 2001, 235, 310

37. “Chemical principles”/Zumdahl, 3.Ed.

38. “Experimental Methods in Polymer Science”/T. Tanaka/Academic Press

39. “Physical Chemistry”/Atkins, 6. Ed.

40.”Invitation to Organic Chemistry”/Bill Johnson, chapter 11

41.”Qantitative chemical Analysis”, 5.Ed./D.C.Harris

42. “An Introduction to Polymer Science”/H.-G. Elias/VCH, 1. Edition, 1997

43. “KJ 439-Kolloidale Systemers statiske og Dynamiske Egenskaper”/Bo Nystrøm,1997

44. “Rheology for Chemists-An Introduction”/J.W. Goodwin, R.W. Hughes/The Royal Society of Chemistry/Cambridge UK, 2000

45. ”Cellulose Ethers, Organic”, “Encyclopaedia of Polymer Science and Technology”, Vol.3

46. “Thermodynamic Properties of Surfactant7Poymer/Water Systems with Respect to Cluster Adsorption and Intermolecular Interaction as a Function of Temperature and Polymer Concentration”/Langmuir, 1997, 13, 1392

47. “Viscosity of Dilute Aqueous Solutions of Hydrophobically Modified Chitosan and its Unmodified Analogue at Different Conditions of Salt and Surfactant Concentrations”/Langmuir, 1997, 13, 4948

48. “On the characterisation principles of some technically important water soluble non-ionic cellulose derivatives”/S. Nilsson et al./Carbohydrate Polymers, 1995, 28, 265

49. “Synthesis and solution behaviour of hydrophobic associating water-soluble polymers containing arylalkyl group”/J. Ma et al. /European Polymer Journal, 2002, 38, 1627

50. “Aggregation Properties of Sodium Hyaluronate with Alkanediyl-α,ω-bis(dimethylalkylammonium bromide) Surfactants in Aqueous Sodium Chloride Solution”/Pisarcik et al./Journal of Colloid and Interface Science, 2000, 228, 207

51. “Mixed Micelles Formed by Cationic Surfactants and Anionic Hydrophobically Modified Polyelectrolytes”/B. Magny, I. Iliopoulos, R. Zana, R. Audebert/Langmuir, 1994,10,3180

52. “Mathematical Statistics and Data Analysis”/John A. Rice, 2. Ed

8. APPENDIX

8.1 Uncertainty-calculations[41]

Uncertainty in the values of the reduced viscosity η_{red} from capillary viscosimetry, $\delta\eta_{red}$, was calculated with equation 26. $\delta\eta_{red}$ was regarded as the standard deviation in reduced viscosity. Equation 26 was derived from equation 25 for η_{red}.

$$25)\ \eta_{red} = (\bar{t} - \bar{t}_0)/\bar{t}_0 \cdot c$$

In equation 26, t and $\bar{t}_0$ (eq. 27) are the mean values in the measured flow times of the solution of HMHEC and the respective solvent through the viscometer in seconds, respectively. c is the concentration of HMHEC in g HMHEC per dl solvent.

26) $\delta\eta_{red} = \eta_{red}\cdot((\delta w/w_p)^2+((\delta w/w_{pl})^2+1/n*(\delta t/\ \bar{t})^2+1/m*(\delta t_0/\ \bar{t_0})^2)^{½}$

δw is the uncertainty in the weighings of polymer and solvent, and is set to 0,0005 g. w_p and w_{pl} are the masses of polymer for the stock solution of HMHEC and the mass of stock solution weighed out for the sample. The term $(\delta w/w_{pl})^2$ was negligible for most solutions, and was neglected, unless for the lowest concentration HMHEC with 3 mmolal 12-6-12. n and m is the number of measurement of flow time on the HMHEC-solution and the respective solvent (pure water, DoTAB (aq), 12-6-12 (aq)), respectively. $\bar{t}$ and $\bar{t_0}$ are calculated from equation 30[41]:

27) $t = (1/n)\cdot\Sigma t_i\ ,\quad \bar{t_0} = (1/m)\cdot\Sigma t_{i,0}$

In equation 27, t_i and $t_{i,0}$ is time measurement i for solution and solvent, n and m is the number of measurement of flow time for solution and the pure solvent.

δt and δt_0 are the measured standard deviation in the flow time through the viscometer, of the solution of HMHEC and the respective solvent for the solution (pure water, DoTAB (aq) or 12-6-12 (aq)),respectively. δt and δt_0 are calculated from equation 31[41].

28) $\delta t = (\Sigma(t_i-\ \bar{t})^2/(n-1))^{½}\ ,\ \delta t_0 = (\Sigma(t_{i,0}-\ \bar{t_0})^2/(m-1))^{½}$

The uncertainty in the values of Huggins constant (table 12) were calculated from

29) $\delta k_H/k_H = ((\delta B/B)^2+4*(\delta A/A)^2)^{½}$

In equation 29, B and A are the constants in the regression lines of reduced viscosity, $\eta_{red}=A+B\cdot c$ (5.3.2.4.), and δB and δA are the uncertainties in the values obtained from the regression (table 11). The uncertainty in intrinsic viscosity $[\eta]$ is

30) $\delta[\eta]=\delta A.$

The uncertainty δc^* in overlapping concentration c^* for the different solutions of HMHEC was calculated from:

31) $\delta c^* = \delta A/A^2$

The values of δc^* are in table 12.The zero shear viscosity η_0 was calculated with equation 32:

32) $\bar{\eta}_0 = (1/k)\cdot\Sigma\eta_j$

In equation 32, η_j is the j. value of shear viscosity in the Newtonian plateau, and k is the number of values of shear viscosity in the Newtonian plateau.
The standard deviation $s(\eta_0)$ in zero shear viscosity η_0 (table 15) is determined from equation 33.

33) $s(\eta_0) = (\Sigma(\eta_j-\ \bar{\eta}_0\ )^2/(k-1))^{½}$

The error bars in the plot of η_0 vs surfactant concentration in figure c, is 97,5% confidence intervals about the mean-value of η_0. The confidence intervals were calculated with equation 34:

$$34)\ \mu = \bar{\eta}_0 \pm t \cdot s(\eta_0)/\sqrt{k}$$

The confidence interval μ in η_0 (eq. 34) is described by the mean value of η_0 (η_0), the standard deviation in η_0 ($s(\eta_0)$), the number of measurements (k), and the value of t from Students t-test[52].

The variation in temperature (mean value $\bar{t}$ and standard deviation in t) for the measurements in capillary viscosimetry are given in table 8.

8.2 Tables

Table 1: Amounts of reagents for hydrophobic modification on HEC.

DMA	HEC	Water	NaOH	$CH_3(CH_2)_{13}Br$
600 ml	11,9563 g	21,19 g	1,7699 g	12,2611 g

Table 2: Amounts of reagents and yields for synthesis of 12-6-12 and 12-φ-12. The data in row 3 are for synthesis a) and data in row 4 are for synthesis b).

	12-6-12			12-φ-12		
Synthesis	N,N-dimethyl dodecylamine	$Br(CH_2)_6Br$	Yield	N,N-dimethyl dodecylamine	$BrCH_2PhCH_2Br$	Yield
a)	3,4242 g	1,8566	30%	1,0375 g	0,5435 g	*
b)	37,3680 g	18,5593 g	40%	32,4864 g	20,1031 g	81%

*No data

Table 3: Samples for ^{1}H NMR

Compound	W (compound)/g	Solvent	W(solvent)/g	[compound]/w/w %
12-6-12	0,0141	$CDCl_3$	1,107	1,3
12--φ-12	0,0149	$CDCl_3$	1,084	1,4
HEC (Natrosol)	0,0508	D_2O	1	5
HMHEC 2	0,0146	DMF-d_7	0,788	1,8

Table 4: The table show the measured melting points T_m in °C of 12-6-12 and 12-φ-12. The measurements (row 3 and 4) were read off as intervals. The calculated means with standard deviations for each synthesis are in 5. row. The means with standard error s for each surfactant are in last row. This standard error was calculated from $s = \sqrt{(s_1^2 + s_2^2)}$, s_1 and s_2 are standard error in T_m for synthesis 1 and 2, respectively.

12-6-12		12-φ-12	
Synthesis 1a)	Synthesis 2a)	Synthesis 1b)	Synthesis 2b)
223-224	222-223	233-234	227,5-229,5
223-226	225-227	231-234	227-228

224±1,4	224±2,2	233±1,4	228±1,1
224±2,6		231±1,8	

Table 5: Data (shift value, integral, estimated number of protons and I/p) obtained from ^1H NMR spectra for hexanediyl-1,6-bis(dimethyldodecylammonium bromide) (12-6-12). The shifting protons are in cursive.

Type of ^1H	chloroform	N+CH$_2$R	N+CH$_2$R	N+CH$_3$	acetone	N+CH$_2$CH$_2$	N+(CH$_2$)$_2$CH$_2$	N+CH$_2$CH$_2$R	RCH$_2$ R´	CH$_3$R
δ (ppm)	7,2	3,7	3,45	3,35	2	1,65	1,55	1,3	1,2	0.85
Integral (I)	-	0,054	0,058	0,148	-	0,050	0,054	0,105	0,372	0,084
No. of ^1H (p)	-	4	4	12	-	4	4	8	32	6
I/p	-	0,0135	0,0145	0,0123	-	0,0125	0,0135	0,0131	0,0116	0,014

Table 6: Data (shift value, integral, estimated number of protons and I/p) obtained from ^1H NMR spectra for dimethylparaphenyl-α,ω-bis(dimethyldodecylammonium bromide) (12-φ-12). The shifting protons are in cursive.

Type of ^1H	chloroform	N+CH$_2$R	N+CH$_2$R	N+CH$_3$	acetone	N+CH$_2$CH$_2$	N+(CH$_2$)$_2$CH$_2$	N+CH$_2$CH$_2$R	RCH$_2$ R´	CH$_3$R
δ (ppm)	7,24	3,7	3,45	3,35	1,98	1,68	1,55	1,3	1,2	0.85
Integral (I)	-	0,054	0,058	0,148	-	0,050	0,054	0,105	0,372	0,084
No.of ^1H (p)	-	4	4	12	-	4	4	8	32	6
I/p	-	0,0135	0,0145	0,0123	-	0,0125	0,0135	0,0131	0,0116	0,014

Table 7 (a-n): Measured values of flow time through a ubbelohde capillary viscometer for different HMHEC in water with and without surfactant. The measurements were done at 25 °C. The tables show a)HMHEC 2/water, b)HMHEC/water, c)HMHEC/1,5 mmolal DoTAB, d) HMHEC/3 mmolal DoTAB, e)HMHEC/6 mmolal DoTAB, f)HMHEC/10 mmolal DoTAB, g)HMHEC/18 mmolal DoTAB, h)HMHEC/20 mmolal DoTAB, i)HMHEC/0,15 mmolal 12-6-12, j) HMHEC/0,2 mmolal 12-6-12, k) HMHEC/1,2 mmolal 12-6-12, l) HMHEC/1,5 mmolal 12-6-12, m) HMHEC/3 mmolal 12-6-12, n) HMHEC/6 mmolal 12-6-12.

a)

HMHEC 2	
c HMHEC g/dl	t/s
0	175,5
	175,4
	175,4

b)

HMHEC	
c HMHEC g/dl	t/s
0	175,4
	175,5
	175,4

c)

1,5 mmolal DoTAB	
c HMHEC g/dl	t/s
0	175,3
0	175,2
	177,2

d)

3 mmolal DoTAB	
c HMHEC g/dl	t/s
0	175,0
3mmolal DoTAB	177,6
	177,9

	175,5		175,5	1,5	177,2		177,9
0,0308	201,8	0,0295	200,8	mmolal	177,6		177,7
	201,8		200,9	DoTAB	177,5		178,7
	201,7		200,7		177,8		178,5
	201,7		200,5	0	175,5	0	175,2
0	175,3		200,8	0	175,5	0,0286	198,6
	175,4	0	175,7	0	175,4		198,6
0,0501	219,7	0,0493	221,2	0,0312	201,6		198,4
	219,7		221,5		201,6		198,6
	219,6		221,7		201,9		198,4
	219,5		221,3		201,8	0	175,1
	219,6		221,4		201,5	0,0536	223,4
0	175,7	0	175,6		201,7		223,4
0,0695	239,0	0,0687	245,6	0	177,3		223,6
	238,9		245,3		177,3		223,2
	239,0		245,2	0,0514	222,0		223,3
	239,0		245,6		221,7	0	175,1
0	175,6		245,8		222,1	0,0719	244,2
0,08996	260,9		245,5		221,7		244,1
	260,9	0	175,5		221,5		244,1
	261,1	0,0882	271,9		221,7		244,3
	261,1		272,0	0	175,2		244,3
	261,0		271,7		175,4	0	175,1
0	175,5		271,4	0,0710	245,6	0,1013	285,3
0,1074	281,0		271,3		245,5		285,3
	280,8	0	175,4		245,2		285,3
	280,9	0,1077	301,6		245,4		285,2
	281,1		301,5		245,3		285,2
	280,9		301,6		245,4	0	175,1
		0,1077	301,3	0	175,7	0,1080	295,9
		0,1077	301,2	0	175,7	0,1080	295,4
				0,0852	263,8		295,6
					263,9		295,9
					263,8		295,6
					263,6		
					263,6		
					263,6		
				0	175,7		
					175,7		
				0,1128	306,5		
					307,0		
					306,8		
					306,7		
					306,9		
					306,8		

e)	f)	g)	h)
6 mmolal DoTAB	10 mmolal DoTAB	18 mmolal DoTAB	20 mmolal DoTAB

c HMHEC g/dl	t/s	c HMHEC g/dl	t/s	c HMHEC g/dl	t/s	c HMHEC g/dl	t/s
0	175,4	0	175,2	0	175,3	0	175,1
6 mmolal DoTAB	178,6		175,3		175,3		175,3
	178,4		175,1	18 mmolal DoTAB	180,2	20 mmolal DoTAB	179,9
	178,4	10 mmolal DoTAB	179,0		180,2		180,0
	178,5		178,3		179,3		180,3
	178,4		178,3		179,4		180,1
	178,5		178,3		179,2		180,1
0	175,3		178,8		179,4		179,9
	175,3		178,9		179,2		180,0
0,0275	195,6		178,7	0	174,9	0	175,3
	195,7	0	175,3		174,8		175,3
	195,5		175,3	0,0346	189,9	0,0254	203,1
	195,4	0,0312	187,8		189,7		203,0
	195,4		187,4		189,9		203,2
0	175,3		187,6		190,0		203,1
	175,3		187,6		175,6		203,2
0,0425	207,4		187,8		175,3		203,2
	207,5		187,6	0	209,6	0	175,4
	207,3		187,7	0,046 4	209,6		175,3
	207,3	0	175,5		209,6		175,4
	207,3		175,2		209,6	0,0379	216,0
	207,3	0,0518	194,4		209,5		216,1
0	175,3		194,5		209,6		216,1
	175,2		194,7		175,4		216,2
0,0663	230,1		194,5		222,1		216,2
	230,3		194,6	0	222,6	0	175,1
	230,3		194,6		222,1		175,2
	230,3		194,5	0,0765	222,4	0,0700	254,3
	230,2	0	175,3		222,2		254,2
	230,2	0,0688	201,5		222,3		254,4
0	175,2		201,4		222,2		254,6
	175,1		201,5		175,3		254,5
	175,7		201,4		175,3		254,5
	175,2		201,4		261,8		254,4
0,0922	259,5		201,4	0	262,0		254,4
	259,7		201,3	0,0907	262,3		254,5
	259,8	0	175,4		261,9		254,6
	259,8		175,4		262,2		254,6
0,0922	259,6	0,0998	214,2	0,0907	261,9	0	175,2
0	175,5		213,8		261,8		175,3
	175,4		214,0	0	175,3	0,0943	289,4
	175,4		213,8		285,4		289,5
	175,4		213,7		285,4		289,5
0,1057	277,5		213,7	0,0982	285,4		289,5
	277,4		213,9		285,5		289,6
	277,6	0	175,5		285,3	0	175,6

	277,0		175,4		175,2		175,5
	277,2	0,1152	227,1		175,2		175,5
	277,2		226,8	0	175,2	0,1202	342,3
	277,0		226,1		299,5		342,5
	276,9		225,3	0,0141	299,6		342,3
			226,1		299,4		342,4
			225,7		299,2		342,2
			225,2		299,5		342,3
							342,2
						0	175,0
						0,0125	190,5
							190,3
							190,4
							190,5
							190,6
							190,7

i)		j)		k)		l)	
0,15 mmolal 12-6-12		0,2 mmolal 12-6-12		1,2 mmolal 12-6-12		1,5 mmolal 12-6-12	
c HMHEC g/dl	t/s	c HMHEC g/dl	t/s	c HMHEC g/dl	t/s	c HMHEC g/dl	t/s
0	175,3	0	175,1	0	175,2	0	175,3
	175,3	0,2 mmolal 12-6-12	178,1		175,2		175,3
0,15 mmolal 12-6-12	177,6		178,3	1,2 mmolal 12-6-12	178,4	1,5 mmolal 12-6-12	177,1
	177,4		178,0		178,3		177,1
	178,6		178,2		177,9		177,4
	178,1		178,1		178,9		177,2
	177,9		178,0		178,9		177,3
	177,3	0	175,2		178,7		177,1
	177,7	0,0284	195,6		178,6		177,2
	177,7		195,0		178,8	0	175,5
	178,8		195,1	0	175,0		175,5
	177,6		194,9	0,0270	197,1	0,0316	204,9
	176,9		194,8		198,0		205,0
0	175,5		194,9		197,4		205,0
	175,5	0	174,9		197,2		205,0
	175,4	0,0537	217,0		197,2		205,0
0,0316	200,2		217,2		197,5		205,1
	199,4		217,5		197,3		205,0
	199,4		217,1	0,0501	221,0	0	175,4
	199,4		217,2		220,9		175,3
	199,5		217,1		220,8	0,0474	223,3
	199,4	0	175,0		220,8		223,2
	199,5	0,0726	237,8		220,7		223,1
0	175,4		237,9		220,8		223,1
	175,3		237,8	0	175,1		223,2
0,0558	223,4		237,9		175,0		223,2
	223,3		238,2	0,0725	253,8		223,2

	223,3	0	175,1		253,7	0	175,3
0,0558	223,3	0,0937	265,5	0,0725	252,5	0,0927	290,9
	223,3		265,9		252,4		291,0
	223,2		265,6		252,5		291,0
	223,2		265,4		254,1		291,1
0	175,4		265,7		253,4		291,4
	175,3	0	175,1	0	175,2		291,2
0,0759	247,8	0,1080	286,7	0,0948	294,0		291,2
	247,9		287,1		294,1	0	175,5
	247,9		287,5		294,6		175,3
	247,9		288,2		295,4	0,1127	334,8
	247,8		286,9		294,1		334,8
	247,9				294,2		334,6
0	175,3				294,0		334,9
	175,4				294,0		334,8
0,15 mmolal 12-6-12	178,0			0	175,1		334,8
	178,3			0,1143	346,2		334,8
	178,1				346,4	0	175,3
	177,2				346,0	1,5 mmolal 12-6-12	177,3
	177,8				346,4		177,1
	177,7				347,3		177,2
	177,7				345,9		177,2
0	175,4				345,8		177,2
0,0990	282,1			0	174,9		177,1
	282,2			0,0092	182,7		177,2
	282,3				182,7	0	175,3
	282,4				182,7	0,0747	260,7
	282,4				182,8		260,8
	282,3				182,7		260,8
	282,3						260,8
0	175,4						260,8
	175,3						260,8
0,1233	325,2					0	174,8
	325,1					0,0109	185,7
	325,1						185,6
	325,3						185,7
	325,2						185,6
	325,1						185,7
	324,8						

m) n)

3 mmolal 12-6-12		6 mmolal 12-6-12	
c HMHEC g/dl	t/s	c HMHEC g/dl	t/s
0	175,1	0	175,3
3 mmolal 12-6-12	178,6	6 mmolal 12-6-12	181,9
	178,6		182,0
	178,6		181,9
	179,6		181,9
	180,6		182,0
	178,7		182,0
	178,7		181,8
0	175,2	0	175,4
0,0285	205,6		175,3
	205,6	0,0301	212,5
	205,8		212,6
	205,8		212,5
	206,1		212,6
0	174,9		212,6
0,0501	229,1	0	175,2
	230,3	0,0479	232,6
	229,2		232,8
	229,2		232,8
	229,4		232,8
0	175,1		232,8
0,0703	254,7		233,0
	254,5	0	175,4
	254,5	0,0678	257,2
	254,6		257,5
	254,6		257,1
0	175,0		257,5
0,0941	289,6		257,3
	289,6		257,3
	288,7		257,3
	289,9	0	175,3
	290,2	0,0890	286,9
0	175,0		286,9
0,1084	313,3		287,1
	313,2		287,0
	312,4		287,0
	311,6		287,1
	311,4	0	175,3
0	174,8		175,3

0,0052	183,4	0,1135	325,6
	183,2		329,8
	183,2		325,9
	183,2		325,9
	183,3		326,3
	183,4		328,7
			325,8
			325,8
		0	174,7
		0,0214	201,8
			202,1
			202,1
			202,2
			202,3
			202,1

Table 8: Temperature (mean value and standard deviation) for the capillary viscosimetry measurements in table 7.

System	temp (mean)/°C	Number of measurements	temp (standard deviation)/ °C
HMHEC 2	24,99	27	$0{,}01_7$
HMHEC	25,01	30	$0{,}02_3$
HMHEC/1,5 mmolal DoTAB	25,00	35	$0{,}00_9$
HMHEC/3 mmolal DoTAB	25,01	31	$0{,}00_6$
HMHEC/6 mmolal DoTAB	24,99	36	$0{,}00_9$
HMHEC/10 mmolal DoTAB	25,00	42	$0{,}01_7$
HMHEC/18 mmolal DoTAB	25,00	41	$0{,}00_6$
HMHEC/20 mmolal DoTAB	25,00	47	$0{,}00_8$
HMHEC/0,15 mmolal 12-6-12	25,00	52	$0{,}00_7$
HMHEC/0,2 mmolal 12-6-12	25,01	34	$0{,}00_7$
HMHEC/1,2 mmolal 12-6-12	25,00	48	$0{,}00_7$
HMHEC/1,5 mmolal 12-6-12	25,00	53	$0{,}00_8$
HMHEC/3 mmolal 12-6-12	25,00	38	$0{,}00_7$
HMHEC/6 mmolal 12-6-12	25,00	45	$0{,}01_2$

Table 9: Calculated values of mean flow time $\bar{t}$, standard deviation in flow time (s_t), number of repetitions of the flow time (n), reduced viscosity (η_{red}) and uncertainty in viscosity η_{red} , ($\delta\eta_{red}$) for solutions with HMHEC-concentrations c, based on the capillary viscosimetric measurements in table 7 for HMHEC/DoTAB.

Solution	c (g/dl)	$\bar{t}$ (s)	s_t (s)	n	η_{red} (dl/g)	$\delta\eta_{red}$(dl/g)
water	0	175,5	$0,0_4$	4	-	-
HMHEC 2	0,0308	201,7	$0,0_4$	4	4,85	$0,01_3$
	0,0501	219,6	$0,1_0$	5	5,02	$0,01_3$
	0,0695	239,0	$0,0_4$	4	5,21	$0,01_4$
	0,0900	261,0	$0,0_7$	5	5,42	$0,01_4$
	0,1074	280,9	$0,1_1$	5	5,60	$0,01_5$
water	0	175,5	$0,0_6$	4	-	-
HMHEC	0,0295	200,7	$0,1_4$	5	4,89	$0,01_0$
	0,0493	221,4	$0,1_8$	5	5,32	$0,01_1$
	0,0687	245,5	$0,2_1$	6	5,81	$0,01_2$
	0,0882	271,6	$0,3_3$	5	6,21	$0,01_3$
	0,1077	301,4	$0,1_9$	5	6,67	$0,01_4$
1,5 mmolal DoTAB	0	177,5	$0,2_4$	5	-	-
1,5 mmolal DoTAB/ HMHEC	0,0312	201,7	$0,1_7$	6	4,37	$0,01_1$
	0,0514	221,8	$0,2_3$	6	4,86	$0,01_2$
	0,0710	245,4	$0,1_2$	6	5,39	$0,01_3$
	0,0852	263,7	$0,1_5$	6	5,70	$0,01_4$
	0,1128	306,8	$0,1_8$	6	6,46	$0,01_6$
3 mmolal DoTAB	0	178,1	$0,4_5$	6	-	-
3 mmolal DoTAB/ HMHEC	0,0286	198,5	$0,1_0$	5	4,01	$0,01_2$
	0,0536	223,4	$0,1_6$	5	4,75	$0,01_4$
	0,0719	244,2	$0,1_0$	5	5,17	$0,01_5$
	0,1013	285,3	$0,0_4$	5	5,95	$0,01_7$
	0,1080	295,7	$0,2_1$	5	6,12	$0,01_8$
6 mmolal DoTAB	0	178,5	$0,0_8$	6	-	-
6mmolal DoTAB/ HMHEC	0,0275	195,5	$0,1_4$	5	3,47	$0,00_9$
	0,0425	207,3	$0,1_0$	6	3,80	$0,01_0$
	0,0663	230,2	$0,1_1$	6	4,37	$0,01_1$
	0,0922	259,7	$0,1_1$	5	4,93	$0,01_3$
	0,1057	277,2	$0,2_4$	8	5,24	$0,01_3$
10 mmolal	0	178,6	$0,2_9$	7	-	-

DoTAB						
10 mmolal DoTAB/ HMHEC	0,0312	187,6	$0,1_4$	7	1,62	$0,00_4$
	0,0518	194,5	$0,0_8$	7	1,72	$0,00_4$
	0,0688	201,4	$0,0_7$	7	1,85	$0,00_5$
	0,0998	213,9	$0,1_7$	7	1,98	$0,00_5$
	0,1152	226,1	$0,7_1$	7	2,31	$0,00_7$
18 mmolal DoTAB	0	179,6	$0,4_3$	7	-	-
18 mmolal DoTAB/ HMHEC	0,0141	189,9	$0,1_4$	6	4,06	$0,01_1$
	0,0346	209,6	$0,0_3$	7	4,82	$0,01_3$
	0,0464	222,3	$0,1_9$	7	5,13	$0,01_4$
	0,0765	262,0	$0,2_0$	5	6,00	$0,01_6$
	0,0907	285,4	$0,0_5$	5	6,50	$0,01_7$
	0,0982	299,4	$0,1_3$	4	6,79	$0,01_8$
20 mmolal DoTAB	0	180,0	$0,1_3$	7	-	-
20 mmolal DoTAB/ HMHEC	0,0125	190,5	$0,1_2$	6	4,63	$0,01_2$
	0,0254	203,1	$0,0_6$	5	5,04	$0,01_3$
	0,0379	216,1	$0,0_6$	11	5,29	$0,01_3$
	0,0700	254,5	$0,1_1$	5	5,90	$0,01_5$
	0,0943	289,5	$0,1_0$	7	6,45	$0,01_6$
	0,1202	342,3	$0,1_1$	6	7,50	$0,01_9$

Table 10: Calculated values of mean flow time $\bar{t}$, standard deviation in flow time (s_t), number of repetitions of the flow time (n), reduced viscosity (η_{red}) and uncertainty in viscosity η_{red} , ($\delta\eta_{red}$) for solutions with HMHEC 1 concentrations c, based on the capillary viscosimetric measurements in table 7 for HMHEC/12-6-12.

Solution	c (g/dl)	$\bar{t}$ (s)	s_t (s)	n	η_{red} (dl/g)	$\delta\eta_{red}$(dl/g)
0,15 mmolal 12-6-12	0	177,8	$0,5_5$	11	-	-
HMHEC/ 0,15 mmolal 12-6-12	0,0316	199,6	$0,3_0$	7	3,88	$0,01_0$
	0,0558	223,3	$0,0_7$	7	4,59	$0,01_2$
	0,0759	247,9	$0,0_7$	6	5,19	$0,01_4$
0,15 mmolal 12-6-12	0	177,8	$0,3_7$	7	-	-
HMHEC/ 0,15 mmolal 12-6-12	0,0990	282,3	$0,1_0$	7	5,94	$0,01_5$
	0,1233	325,1	$0,1_4$	7	6,72	$0,01_7$
0,2 mmolal	0	178,1	$0,1_1$	7	-	-

12-6-12						
HMHEC/ 0,2 mmolal 12-6-12	0,0284	195,0	$0,2_9$	6	3,35	$0,00_9$
	0,0537	217,2	$0,1_7$	6	4,09	$0,01_1$
	0,0726	237,9	$0,1_3$	5	4,63	$0,01_2$
	0,0937	265,6	$0,1_9$	5	5,25	$0,01_4$
	0,1080	287,3	$0,6_2$	5	5,67	$0,01_6$
1,2 mmolal 12-6-12	0	178,6	$0,3_4$	8	-	-
HMHEC/ 1,2 mmolal 12-6-12	0,0092	182,7	$0,0_4$	7	2,52	$0,00_7$
	0,0270	197,4	$0,3_1$	6	3,90	$0,01_1$
	0,0501	220,8	$0,1_1$	7	4,73	$0,01_3$
	0,0725	253,2	$0,6_9$	8	5,76	$0,01_7$
	0,0948	294,3	$0,5_0$	7	6,84	$0,02_0$
	0,1143	346,3	$0,5_1$	5	8,22	$0,02_4$
1,5 mmolal 12-6-12	0	177,2	$0,1_2$	7	-	-
HMHEC/ 1,5 mmolal 12-6-12	0,0109	185,6	$0,0_6$	7	4,40	$0,01_1$
	0,0316	205,0	$0,0_6$	6	4,97	$0,01_2$
	0,0474	223,2	$0,0_6$	7	5,48	$0,01_4$
	0,0747	260,8	$0,0_4$	7	6,32	$0,01_6$
1,5 mmolal 12-6-12	0	177,2	$0,0_7$	7	-	-
HMHEC/ 1,5 mmolal 12-6-12	0,0927	291,1	$0,1_8$	7	6,93	$0,01_7$
	0,1127	334,8	$0,1_0$	5	7,89	$0,02_0$
3 mmolal 12-6-12	0	179,1	$0,7_7$	7	-	-
HMHEC/ 3 mmolal 12-6-12	0,0052	183,3	$0,0_9$	5	4,53	$0,01_5$
	0,0285	205,8	$0,2_0$	5	5,24	$0,01_7$
	0,0501	229,4	$0,4_8$	5	5,61	$0,01_9$
	0,0703	254,6	$0,0_8$	5	6,00	$0,01_9$
	0,0941	289,6	$0,5_9$	5	6,56	$0,02_2$
	0,1084	312,4	$0,8_6$	6	6,87	$0,02_4$
6 mmolal 12-6-12	0	181,9	$0,0_7$	7	-	-
HMHEC/ 6 mmolal 12-6-12	0,0214	202,1	$0,1_6$	5	5,17	$0,01_4$
	0,0301	212,6	$0,0_3$	6	5,59	$0,01_5$
	0,0479	232,8	$0,1_4$	7	5,83	$0,01_5$
	0,0678	257,3	$0,1_3$	6	6,11	$0,01_6$
	0,0890	287,0	$0,0_9$	8	6,49	$0,01_7$
	0,1135	326,7	$1,6_1$	6	7,01	$0,02_2$

Table 11: Constants (A, B) for linear regression lines (Y=A+B*X) for reduced viscosity (table 9 and 10) for aqueous solutions of HMHEC in water and with dodecyltrimethylammonium bromide (DoTAB) and hexanediyl-1,6-bis(dimethyldodecylammonium bromide) (12-6-12).

Solution	c (surfactant)	A (dl/g)	δA (dl/g)	B (dl^2/g^2)	δB (dl^2/g^2)
HMHEC 2	0	4,54	$0,01_6$	9,7	$0,2_2$
HMHEC	0	4,22	$0,01_3$	22,8	$0,1_9$
HMHEC/1,5 mmolal DoTAB	1,5139	3,57	$0,01_4$	25,4	$0,2_1$
HMHEC/3 mmolal DoTAB	2,9810	3,28	$0,01_6$	26,4	$0,2_2$
HMHEC/6 mmolal DoTAB	5,9955	2,85	$0,01_1$	22,6	$0,1_7$
HMHEC/10 mmolal DoTAB	10,1192	1,38	$0,00_5$	6,9	$0,0_8$
HMHEC/18 mmolal DoTAB	17,5159	3,65	$0,01_1$	31,6	$0,1_9$
HMHEC/20 mmolal DoTAB	19,9920	4,35	$0,01_0$	24,0	$0,1_6$
HMHEC/0,15 mmolal 12-6-12	0,1492	2,88	$0,01_4$	30,8	$0,1_9$
HMHEC/0,2 mmolal 12-6-12	0,1997	2,52	$0,01_3$	29,1	$0,1_9$
HMHEC/1,2 mmolal 12-6-12	1,1694	2,14	$0,00_7$	51,8	$0,1_6$
HMHEC/1,5 mmolal 12-6-12	1,5096	3,98	$0,01_0$	32,7	$0,1_7$
HMHEC/3 mmolal 12-6-12	3,0590	4,48	$0,01_3$	22,2	$0,2_1$
HMHEC/6 mmolal 12-6-12	5,9965	4,90	$0,01_3$	18,4	$0,2_2$

Table 12: Calculated values of intrinsic viscosity ([η]), uncertainty in reduced viscosity (δ[η]), Huggins constant (k_H), uncertainty in k_H (δk_H) and overlapping concentration c* with uncertainty (δc*) for different HMHEC concentrations c for aqueous solutions of HMHEC, HMHEC 2, HMHEC/DoTAB, and HMHEC/12-6-12 and without surfactant based on the constants (A, B) from the regression lines in table 11.

Solution	c(mmolal)	[η] (dl/g)	δ[η] (dl/g)	k_H	δk_H	c* (g/dl)	δc* (g7dl)
HMHEC 2	0	4,54	$0,01_6$	0,47	$0,01_1$	0,220	$0,000_8$
HMHEC	0	4,22	$0,01_3$	1,28	$0,01_3$	0,237	$0,000_7$
HMHEC/1,5 mmolal DoTAB	1,5139	3,57	$0,01_4$	2,00	$0,02_3$	0,280	$0,001_1$
HMHEC/3 mmolal DoTAB	2,9810	3,28	$0,01_6$	2,45	$0,03_1$	0,305	$0,001_4$
HMHEC/6 mmolal DoTAB	5,9955	2,85	$0,01_1$	2,78	$0,03_0$	0,351	$0,001_3$
HMHEC/10 mmolal DoTAB	10,1192	1,38	$0,00_5$	3,59	$0,04_8$	0,723	$0,002_8$

HMHEC/18 mmolal DoTAB	17,5159	3,65	$0,01_1$	2,38	$0,02_0$	0,274	$0,000_8$
HMHEC/20 mmolal DoTAB	19,9920	4,35	$0,01_0$	1,27	$0,01_0$	0,230	$0,000_5$
HMHEC/0,15 mmolal 12-6-12	0,1492	2,88	$0,01_4$	3,71	$0,04_2$	0,347	$0,001_7$
HMHEC/0,2 mmolal 12-6-12	0,1997	2,52	$0,01_3$	4,56	$0,05_4$	0,396	$0,002_0$
HMHEC/1,2 mmolal 12-6-12	1,1694	2,14	$0,00_7$	11,28	$0,08_3$	0,467	$0,001_6$
HMHEC/1,5 mmolal 12-6-12	1,5096	3,98	$0,01_0$	2,06	$0,01_5$	0,251	$0,000_6$
HMHEC/3 mmolal 12-6-12	3,0590	4,48	$0,01_3$	1,10	$0,01_2$	0,223	$0,000_6$
HMHEC/6 mmolal 12-6-12	5,9965	4,90	$0,01_3$	0,77	$0,01_0$	0,204	$0,000_6$

Table 13: Rheological measurements of shear viscosity with increasing shear rate performed with a Physica MCR 300 rheometer, with a MCR300 SN510080 measuring device. The measurements were done with 0,75wt% aqueous solutions of HMHEC with dodecyltrimethylammonium bromide (DoTAB). Temperature 25°C. The measurements were carried out with a cone-plate 7,5 cm -1° measuring system

HMHEC/5mmolal DoTAB		HMHEC/10mmolal DoTAB		HMHEC/ 15 mmolal DoTAB		HMHEC/ 20 mmolal DoTAB	
Shear rate (1/s)	Shear viscosity (Pa·s)	Shear rate (1/s)	Shear viscosity (Pa·s)	Shear rate (1/s)	Shear viscosity (Pa·s)	Shear rate (1/s)	Shear viscosity (Pa·s)
0,1	0,194	0,05	0,516	0,01	1,16	0,01	0,208
0,137	0,197	0,0704	0,514	0,0149	1,14	0,0149	0,225
0,189	0,193	0,099	0,504	0,0221	1,09	0,0221	0,236
0,259	0,189	0,139	0,495	0,0329	1,04	0,0329	0,239
0,356	0,187	0,196	0,486	0,0489	0,994	0,0489	0,239
0,489	0,186	0,276	0,48	0,0728	0,964	0,0728	0,233
0,672	0,184	0,388	0,47	0,108	0,949	0,108	0,224
0,924	0,182	0,546	0,461	0,161	0,941	0,161	0,215
1,27	0,18	0,768	0,451	0,239	0,943	0,24	0,208
1,74	0,178	1,08	0,442	0,356	0,947	0,356	0,204
2,39	0,175	1,52	0,433	0,53	0,944	0,53	0,2
3,29	0,172	2,14	0,423	0,788	0,931	0,788	0,197
4,52	0,169	3,01	0,411	1,17	0,913	1,17	0,196
6,21	0,166	4,24	0,396	1,74	0,891	1,74	0,193
8,53	0,162	5,96	0,376	2,59	0,855	2,59	0,191
11,7	0,158	8,39	0,35	3,86	0,779	3,86	0,187
16,1	0,153	11,8	0,317	5,74	0,696	5,74	0,183
22,1	0,145	16,6	0,283	8,53	0,623	8,53	0,181
30,4	0,135	23,4	0,248	12,7	0,564	12,7	0,178
41,8	0,121	32,9	0,216	18,9	0,489	18,9	0,175
57,4	0,107	46,3	0,188	28,1	0,448	28,1	0,172
78,8	0,0946	65,1	0,163	41,8	0,4	41,8	0,168

108	0,083	91,6	0,141	62,1	0,337	62,1	0,164
149	0,0724	129	0,122	92,4	0,283	92,4	0,159
204	0,0627	181	0,105	137	0,232	137	0,152
281	0,0541	255	0,0897	204	0,186	204	0,143
386	0,0466	359	0,0765	304	0,146	304	0,135
530	0,04	505	0,0651	452	0,14	452	0,124
728	0,0344	711	0,0549	672	0,118	672	0,108
1 000	0,0295	1 000	0,0456	1 000	0,0837	1 000	0,0889

Table 14: Rheological measurements of shear viscosity with increasing shear rate performed with a Physica MCR 300 rheometer, with a MCR300 SN510080 measuring device. The measurements were done with 0,75wt% aqueous solutions of HMHEC with and without hexanediyl-1,6-bis(dimethyldodecylammonium bromide) (12-6-12). Temperature 25°C. The measurements were carried out with a cone-plate 7,5 cm -1° measuring system

HMHEC/water		HMHEC/ 0,15 mmolal 12-6-12		HMHEC/0,6 mmolal 12-6-12		HMHEC/ 0,75 mmolal 12-6-12	
Shear rate (1/s)	Shear viscosity (Pa·s)	Shear rate (1/s)	Shear viscosity (Pa·s)	Shear rate (1/s)	Shear viscosity (Pa·s)	Shear rate (1/s)	Shear viscosity (Pa·s)
0,5	0,0799	0,1	0,085	0,1	0,187	0,05	0,33
0,65	0,0796	0,137	0,086	0,137	0,188	0,0704	0,33
0,845	0,0793	0,189	0,0862	0,189	0,188	0,099	0,33
1,1	0,079	0,259	0,0859	0,259	0,183	0,139	0,329
1,43	0,0786	0,356	0,086	0,356	0,18	0,196	0,328
1,85	0,078	0,489	0,0855	0,489	0,176	0,276	0,326
2,41	0,0774	0,672	0,0845	0,672	0,173	0,388	0,323
3,13	0,0766	0,924	0,084	0,924	0,17	0,546	0,32
4,07	0,0758	1,27	0,0832	1,27	0,166	0,768	0,317
5,29	0,0748	1,74	0,0823	1,74	0,162	1,08	0,313
6,87	0,0739	2,4	0,0814	2,4	0,159	1,52	0,309
8,93	0,0729	3,29	0,0802	3,29	0,156	2,14	0,304
11,6	0,072	4,52	0,079	4,52	0,152	3,01	0,298
15,1	0,0712	6,21	0,0778	6,21	0,149	4,24	0,293
19,6	0,0705	8,53	0,0764	8,53	0,146	5,96	0,287
25,5	0,0697	11,7	0,0751	11,7	0,142	8,39	0,28
33,1	0,0686	16,1	0,0739	16,1	0,137	11,8	0,27
43,1	0,0667	22,1	0,0726	22,1	0,131	16,6	0,255
56	0,0637	30,4	0,0709	30,4	0,123	23,4	0,236
72,7	0,0593	41,8	0,0682	41,8	0,112	32,9	0,214
94,5	0,054	57,4	0,0639	57,4	0,1	46,3	0,191
123	0,0482	78,8	0,058	78,8	0,088	65,1	0,17
160	0,0427	108	0,0512	108	0,0769	91,6	0,149
208	0,038	149	0,0444	149	0,0669	129	0,129
270	0,034	204	0,0385	204	0,0579	181	0,112
350	0,0302	281	0,0335	281	0,0499	255	0,0969
456	0,0269	386	0,0292	386	0,0427	359	0,0834
592	0,0239	530	0,0254	530	0,0363	505	0,0714
769	0,0212	728	0,0221	728	0,031	711	0,061

1 000	0,0188	1 000	0,0192	1 000	0,0265	1 000	0,0518

Table 14, continued.

HMHEC/ 1,5 mmolal 12-6-12		HMHEC/ 3 mmolal 12-6-12		HMHEC/ 6 mmolal 12-6-12		HMHEC/ 12 mmolal 12-6-12	
Shear rate (1/s)	Viscosity (Pa·s)	Shear rate (1/s)	Viscosity (Pa·s)	Shear rate (1/s)	Viscosity (Pa·s)	Shear rate (1/s)	Viscosity (Pa·s)
0,01	0,571	0,01	0,158	0,01	0,0529	0,1	0,0248
0,0149	0,555	0,0149	0,161	0,0149	0,0553	0,137	0,0255
0,0221	0,538	0,0221	0,167	0,0221	0,0559	0,189	0,0255
0,0329	0,528	0,0329	0,17	0,0329	0,0561	0,259	0,0258
0,0489	0,52	0,0489	0,172	0,0489	0,0564	0,356	0,0257
0,0728	0,506	0,0728	0,172	0,0728	0,0573	0,489	0,0254
0,108	0,494	0,108	0,171	0,108	0,0577	0,672	0,0254
0,161	0,488	0,161	0,171	0,161	0,0572	0,924	0,0255
0,239	0,48	0,24	0,171	0,24	0,0571	1,27	0,0254
0,356	0,476	0,356	0,171	0,356	0,0569	1,74	0,0254
0,53	0,469	0,53	0,17	0,53	0,0567	2,4	0,0254
0,788	0,461	0,788	0,17	0,788	0,0566	3,29	0,0253
1,17	0,454	1,17	0,169	1,17	0,0566	4,52	0,0254
1,74	0,445	1,74	0,169	1,74	0,0566	6,21	0,0254
2,59	0,436	2,59	0,168	2,59	0,0567	8,53	0,0253
3,86	0,426	3,86	0,167	3,86	0,0567	11,7	0,0253
5,74	0,417	5,74	0,166	5,74	0,0565	16,1	0,0252
8,53	0,409	8,53	0,164	8,53	0,0564	22,1	0,0251
12,7	0,399	12,7	0,162	12,7	0,0562	30,4	0,025
18,9	0,388	18,9	0,159	18,9	0,0558	41,8	0,0248
28,1	0,369	28,1	0,155	28,1	0,0551	57,4	0,0246
41,8	0,344	41,8	0,151	41,8	0,0542	78,8	0,0242
62,1	0,313	62,1	0,147	62,1	0,053	108	0,0238
92,4	0,284	92,4	0,143	92,4	0,0516	149	0,0232
137	0,255	137	0,136	137	0,0498	204	0,0225
204	0,226	204	0,128	204	0,0477	281	0,0218
304	0,195	304	0,12	304	0,0453	386	0,0209
452	0,154	452	0,11	452	0,0423	530	0,0198
672	0,114	672	0,0979	672	0,039	728	0,0186
1 000	0,0967	1 000	0,0834	1 000	0,0354	1 000	0,0174

Table 15: Calculated values of zero shear viscosity η_0 obtained from values of shear viscosity η in table 13 and 14 for HMHEC/water and aqueous solutions of HMHEC with DoTAB or 12-6-12. The numbers in parentheses in 2. column is the number of shear viscosity measurements (counted from the lowest shear value) used in determining the zero shear viscosity mean values $\bar{\eta}_0$ in column 2 for each solution. $s(\eta_0)$ is the standard deviation in η_0.

Solution	$\bar{\eta}_0$ (Pa·s)	$s(\eta_0)$ (Pa·s)	Conc. (DoTAB/12-6-12) (mmolal)
HMHEC	0,079 (8)	$0{,}001_1$	0

HMHEC /0,15 mmolal 12-6-12	0,085 (11)	$0,001_6$	0,1418
HMHEC/0,6 mmolal 12-6-12	0,185 (5)	$0,003_6$	0,5863
HMHEC/0,75 mmolal 12-6-12	0,326 (9)	$0,004_8$	0,7097
HMHEC/1,5 mmolal 12-6-12	0,53 (7)	$0,02_7$	1,4999
HMHEC/3 mmolal 12-6-12	0,166 (22)	$0,006_0$	3,0466
HMHEC/6 mmolal 12-6-12	0,056 (24)	$0,001_5$	6,1656
HMHEC/12 mmolal 12-6-12	0,0252 (23)	$0,0004_7$	12,0735
HMHEC/5 mmolal DoTAB	0,19 (7)	$0,004_8$	5,0021
HMHEC /10 mmolal DoTAB	0,51 (4)	$0,09_7$	10,0860
HMHEC /15 mmolal DoTAB	1,11 (4)	$0,05_4$	15,1375
HMHEC /20 mmolal DoTAB	0,22 (11)	$0,01_5$	20,7277